AD-A145 130 INTERPLANETARY COSMIC RAY INTENSITY: 1972-1984 AND OUT TO 32 AU(U) IOWA UNIV IOWA CITY DEPT OF PHYSICS AND ASTRONOMY J A VAN ALLEN ET AL. AUG 84 U. OF IOWA-84-19 1/1

UNCLASSIFIED N00014-76-C-0016 F/G 4/1 NL

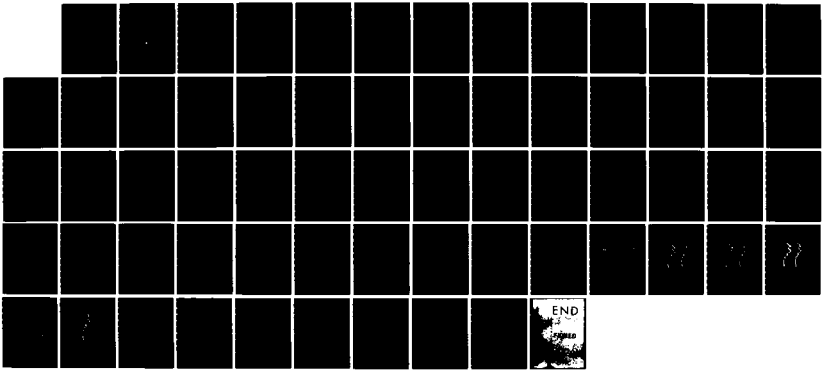

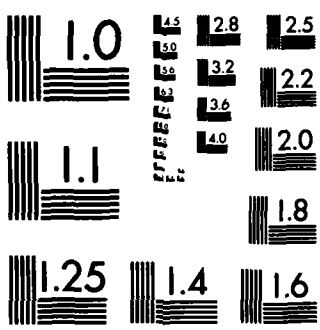

U. of Iowa 84-19

Interplanetary Cosmic Ray Intensity: 1972-1984 and Out to 32 AU

by

J. A. VAN ALLEN and B. A. RANDALL
Department of Physics and Astronomy
University of Iowa
Iowa City, Iowa 52242

Department of Physics and Astronomy
THE UNIVERSITY OF IOWA
Iowa City, Iowa 52242

U. of Iowa 84-19

Interplanetary Cosmic Ray Intensity: 1972-1984 and Out to 32 AU

by

J. A. VAN ALLEN and B. A. RANDALL
Department of Physics and Astronomy
University of Iowa
Iowa City, Iowa 52242

August 1984

Submitted for Publication to J. Geophys. Res.

UNCLASSIFIED

SECURITY CLASSIFICATION OF THIS PAGE (When Data Entered)

REPORT DOCUMENTATION PAGE		READ INSTRUCTIONS BEFORE COMPLETING FORM
1. REPORT NUMBER U. of Iowa 84-19	2. GOVT ACCESSION NO. --	3. RECIPIENT'S CATALOG NUMBER --
4. TITLE (and Subtitle) INTERPLANETARY COSMIC RAY INTENSITY: 1972-1984 AND OUT TO 32 AU		5. TYPE OF REPORT & PERIOD COVERED Progress, August 1984 6. PERFORMING ORG. REPORT NUMBER
7. AUTHOR(s) J. A. Van Allen and B. A. Randall		8. CONTRACT OR GRANT NUMBER(s) N00014-76-C-0016
9. PERFORMING ORGANIZATION NAME AND ADDRESS Department of Physics and Astronomy The University of Iowa Iowa City, Iowa 52242		10. PROGRAM ELEMENT, PROJECT, TASK AREA & WORK UNIT NUMBERS --
11. CONTROLLING OFFICE NAME AND ADDRESS Office of Naval Research Electronics Program Office Arlington, Virginia 22217		12. REPORT DATE August 1984 13. NUMBER OF PAGES 61
14. MONITORING AGENCY NAME & ADDRESS(if different from Controlling Office)		15. SECURITY CLASS. (of this report) UNCLASSIFIED 15a. DECLASSIFICATION/DOWNGRADING SCHEDULE

16. DISTRIBUTION STATEMENT (of this Report)

Approved for public release; distribution is unlimited.

17. DISTRIBUTION STATEMENT (of the abstract entered in Block 20, if different from Report)

18. SUPPLEMENTARY NOTES

To be published in Journal of Geophysical Research.

19. KEY WORDS (Continue on reverse side if necessary and identify by block number)

Cosmic Ray Gradient
Interplanetary Cosmic Rays
Solar Activity Cycle

20. ABSTRACT (Continue on reverse side if necessary and identify by block number)

See pages 2-3 following.

DD FORM 1 JAN 73 1473 EDITION OF 1 NOV 65 IS OBSOLETE
S/N 0102-LF-014-6601

UNCLASSIFIED

SECURITY CLASSIFICATION OF THIS PAGE (When Data Entered)

ABSTRACT

Using a number of Geiger-Mueller tubes in the University of Iowa instruments on Pioneer 10 and Pioneer 11, we have measured the interplanetary intensity of cosmic rays (E_p > 80 MeV) over a complete solar activity cycle and out to a heliocentric distance of over 32 AU. Free space values of the background corrections due to the radioisotope thermal generators were determined during passage of Pioneer 11 under the dense rings of Saturn during the 1 September 1979 encounter. These improved corrections and ones inferred therefrom for Pioneer 10 have supplanted earlier estimates and have been applied to all data.

During the period 1972-1984, intensity vs time curves have a flat, more-or-less constant maximum during 1975, 1976, and 1977; a brief (~ 8 months) minimum in mid-1981; and another brief minimum centered around early January 1983. The ratio of maximum to minimum intensity (normalized to same radial distance) is ≈ 2.7. The temporal correlation of intensity at P10 with that at P11 is good, after allowance for propagation delay, as is that with data from the Deep River Neutron Monitor. The max/min intensity ratio for the latter is ≈ 1.25. As noted by us and others in previous studies, the decline in intensity after the prolonged

maximum occurred primarily by an irregular succession of stepwise decreases with subsequent slow recovery such that successive decreases overlapped cumulatively. The logarithms of the ratios of the counting rates of a GM tube on P10 to that of a matched GM tube on P11 (after allowance for propagation delay) were plotted against the differences in heliocentric radial distance Δr. Three such independent plots were made, one for each of a matched pair of tubes. The three least-squares-fitted trend lines through the entire body of data for each pair of detectors yield integral radial gradients G of +2.00 (± 0.07), +2.07 (± 0.05), and +2.12 (± 0.06) percent per AU. Our adopted mean value with estimated uncertainty for all known causes is

$$G = +2.06\ (\pm\ 0.20)\ \text{percent per AU}$$

for the radial range $1 < r < 32$ AU. The reciprocal of G, namely 50 AU, is the scale length of the heliosphere. By direct observation, the modulating influence of the sun is still clearly present at 32 AU. Hence the radius of the heliospheric modulation region $r_B > 32$ AU. Various arguments, no one of which is convincing, suggest that r_B lies between 50 and 100 AU.

I. INTRODUCTION

This paper gives a progress report on our long term study of the interplanetary intensity of the cosmic radiation out to great distances from the sun using a system of detectors on the spacecraft Pioneer 10 and Pioneer 11. The observations give the integral intensity of cosmic rays having energies sufficient to penetrate the physical shields of the detectors, which correspond to the range of a proton of kinetic energy E_p = 80 MeV or of a helium nucleus of specific kinetic energy ϵ_α = 80 MeV/nucleon. The omnidirectional integral intensity is proportional to the counting rate of a detector.

As of 1 April 1984, the heliocentric distances of the two spacecraft were 32.48 and 15.81 AU, respectively. The Jupiter encounter/heliospheric mission of Pioneer 10 began with launch of the spacecraft on 3 March 1972. Following its encounter with Jupiter in early December 1973, the spacecraft has been on a hyperbolic, escape trajectory from the solar system. The asymptote of this trajectory is at $\lambda_\infty = 83.^\circ3$, $\beta_\infty = +2.^\circ9$ (heliocentric ecliptic longitude and latitude in 1950.0 coordinates) and $v_\infty = 2.39$ AU yr^{-1}. The projected heliocentric distances r during the next ten years are as follows:

35 AU, March 1985; 40 AU, December 1986; 45 AU, November 1988; 50 AU, September 1990; 55 AU, August 1992; and 60 AU, July 1994.

The Jupiter encounter/Saturn encounter/heliospheric mission of Pioneer 11 began with launch on 6 April 1973. This spacecraft encountered Jupiter in early December 1974 and Saturn in late August - early September 1979. Since the latter encounter Pioneer 11 has also been on a hyperbolic, escape trajectory from the solar system with $\lambda_\infty = 290°.2$, $\beta_\infty = +12°.8$, and $v_\infty = 2.20$ AU yr^{-1}. Projected heliocentric distances are as follows: 20 AU, January 1986; 25 AU, January 1988; 30 AU, January 1990; 35 AU, January 1992; and 40 AU, February 1994.

The University of Iowa instruments on both spacecraft continue to operate flawlessly. As Pioneer 11 flew under the rings of Saturn on 1 September 1979 there was a unique opportunity to determine the free-space background counting rates of the detectors caused by the Radioisotope Thermal Generators (RTG's) that furnish electrical power to the spacecraft. The present paper is the first of our series of papers on the interplanetary cosmic ray intensity [Van Allen, 1972; Thomsen and Van Allen, 1974; Van Allen, 1976, 1979, 1980] to use the revised background rates derived from observations during the Saturn encounter. Hence, this paper provides an improvement over previous ones as well as an extension of the study to greater heliocentric distances. (See Appendix I for Remarks on Validity and Accuracy of Data.)

Relevant recent papers using data from various instruments on Pioneers 10 and 11; on the two other outer heliospheric spacecraft Voyagers 1 and 2; and on IMP 7, IMP 8, and Helios 1 and 2 in earth orbit and in the inner heliosphere; and from earth-based neutron monitors are by: Webber and Lockwood [1981], McDonald et al. [1981a]; McDonald et al. [1981b], McKibben et al. [1982], Lockwood and Webber [1984], Venkatesan et al. [1984a], Decker et al. [1984], and Venkatesan et al. [1984b].

The trajectories of Pioneer 10, Pioneer 11, Voyager 1, and Voyager 2 are shown in Figure 1.

II. OBSERVED DATA

Daily mean counting rates of our three matched pairs of detectors are shown as a function of time in Figures 2, 3, and 4. Occasional upward spikes are caused by solar energetic particles. All counting rates have been corrected for temperature and, more importantly, for RTG background (Appendix I). A comparison with the Deep River Neutron Monitor data (daily means) [Solar-Geophysical Data, 1972-1984] is shown in Figure 5. A plot of monthly mean sunspot numbers [Solar-Geophysical Data, 1984] is given in Figure 6 to provide a guide to solar activity for comparison with the sample of Pioneer 10 data. Some general remarks on the observed data are as follows:

1. Figures 2, 3, and 4 show that solar modulation of the cosmic ray intensity extends out at least 32 AU.

2. There is a close resemblance in considerable detail between the intensity-time curves for Pioneer 10 and those for Pioneer 11 throughout the past eleven years (a full solar activity cycle). Identifiable features at P10 are progressively more delayed relative to the corresponding features at P11 as the difference in their heliocentric

distances Δr increases [cf. Van Allen, 1976]. The delay corresponds roughly to the ratio of Δr to 440 km s^{-1}.

3. A pronounced 26-day periodic variation of cosmic ray intensity with amplitude ~ 4% occurred in 1974-76 (solar activity minimum) [Van Allen, 1976] but such periodicity has been difficult, if not impossible, to discern thereafter. The obliteration of the 26-day variation is attributed to an increasing number of active centers on the sun and to an increasing level of roughness in the interplanetary magnetic field.

4. The correlation between the interplanetary intensity of cosmic rays and the counting rate of the high latitude Deep River Neutron Monitor (Figure 5) is impressively good (allowing for propagation delay) despite the fact that the effective primary energy to which the latter responds is several times greater than the effective energy to which our GM tubes respond. A detailed comparison for two great Forbush decreases in mid-1982 is given in Figure 7.

5. In Figure 6 there is seen to be a good general anti-correlation between cosmic ray intensity and sunspot number, the latter being taken as a crude measure of solar activity. During the period 1972-1976 (declining solar activity) the two curves are approximately in phase (± 1 month) but thereafter the cosmic ray intensity lags behind the sunspot number by an increasing amount (increasing solar activity) and

continues to do so during the subsequent period (maximum and declining solar activity). During 1980-1984 the lag is about 1.1 year as illustrated by the portion of the sunspot curve that has been moved to the right by this amount and superimposed on the cosmic ray intensity curve at the right hand end of the latter in Figure 6. The 1.1 year delay is much greater than the solar wind propagation delay from 1 to 30 AU, namely ~ 110 days.

III. RADIAL GRADIENT OF INTENSITY

Making the common, though perhaps incorrect, assumption of spherical symmetry about the sun, the omnidirectional cosmic ray intensity J is a function of two variables -- radial distance r and time t. The detailed temporal tracking of the intensities at P10 and P11 with propagation delay $\Delta t \approx (r_{10} - r_{11})/v_{sw}$ suggests the further assumption that the radial and temporal dependences of J are uncoupled and that J can be written as the product of two separate functions, viz.

$$J_{10}\,(r_{10},\, t + \Delta t) \;=\; K_{10}\, f(r_{10}) \,.\, h(t + \Delta t) \qquad (1)$$

and

$$J_{11}\,(r_{11},\, t) \;=\; K_{11}\, f(r_{11}) \,.\, h(t) \qquad (2)$$

wherein K_{10} and K_{11} are reciprocal geometric factors (reciprocal effective areas) of the respective detectors,

$$\Delta t \;=\; \frac{(r_{10} - r_{11})}{v_{sw}} \;=\; \frac{\Delta r}{v_{sw}}\,, \qquad (3)$$

and v_{sw} is the mean solar wind velocity over Δt.

Then by (1) and (2)

$$\frac{J_{10}(r_{10}, t + \Delta t)}{J_{11}(r_{11}, t)} = \frac{K_{10}}{K_{11}} \frac{f(r_{10})}{f(r_{11})} \cdot \frac{h(t + \Delta t)}{h(t)} \qquad (4)$$

The delayed correlation process (see next section) establishes Δt and, in effect, makes $\frac{h(t + \Delta t)}{h(t)}$ equal to unity, so that

$$\frac{J_{10}(r_{10}, t + \Delta t)}{J_{11}(r_{11}, t)} = K \frac{f(r_{10})}{f(r_{11})} \qquad (5)$$

where $K \equiv K_{10}/K_{11}$. A specific assumption on the form of $f(r)$ is

$$f(r) = \exp(G\, r) . \qquad (6)$$

Then

$$\frac{J_{10}(r_{10}, t + \Delta t)}{J_{11}(r_{11}, t)} = K \exp(G \Delta r) . \qquad (7)$$

G is called the integral radial gradient, usually expressed in percent per AU. The scale length of the radial dependence is 1/G.

IV. ANALYSIS OF DATA

The observed data, as represented by Figures 2, 3, and 4, have been analyzed to determine the dependence of intensity on r. First, each 25-day segment of daily mean counting rates of a detector on P10, say C_{10}, is compared with the simultaneous 25-day segment of daily mean counting rates of the corresponding detector on P11, in this case C_{11}. The ratio C_{10}/C_{11} is computed for each pair of days; then the 25-day mean ratio and the standard deviation of the 25 daily mean ratios from that mean are computed. The process is then repeated by sliding the P10 block of days backwards in time relative to the P11 data in increments of one day to cover the range of delays corresponding to $250 < v_{sw} < 750$ km s^{-1}. The case that yields the lowest value of the standard deviation of the 25 daily mean ratios from the 25-day mean ratio is adopted as establishing the propagation delay Δt and the corresponding 25-day mean ratio. The latter quantity is $f(r_{10})/f(r_{11})$ in equation (5). The delays determined by the above procedure are not of as high an accuracy as was possible during 1974-76 [Van Allen, 1976] but do resemble $\Delta r/v_{sw}$ with a typical value $v_{sw} \sim 440$ km s^{-1}. The "delayed ratios" of B_{10}/B_{11}, C_{10}/C_{11}, and D_{10}/D_{11} are plotted as a function of Δr in Figures 8, 9, and 10. The error bars on the ratios are standard

deviations based on statistics only, with no contribution from the uncertainty in selecting the proper pair of intervals for which the ratio is computed.

The least squares linear fits to these semilog plots are of the form exp ($G \Delta r$). The numerical values of G and their formal standard errors are as follows:

For B_{10}/B_{11}: +2.00 (± 0.07) percent per AU

For C_{10}/C_{11}: +2.07 (± 0.05)

For D_{10}/D_{11}: +2.12 (± 0.06)

The three overall trend lines (Figs. 8, 9, and 10) for the ratios of counting rates of the three independent pairs of detectors have essentially identical slopes. The mean value of the integral radial gradient ($E_p > 80$ MeV) with an estimated uncertainty from all known causes is

$$G = +2.06\ (\pm\ 0.20) \text{ percent per AU, } 1 < r < 32 \text{ AU.} \quad (8)$$

This mean radial gradient is one of the principal results of the present paper. It is derived from data over an eleven-year period. The calculation of the gradient is based on the varying quantity Δr whose greatest value up to 1 April 1984 is 16.7 AU. But because of the assumed form

$$f(r) = \exp (G r), \quad (6)$$

the gradient G has, in effect, been measured piecewise over the range $1 \leq r \leq 32$ AU.

The scale size of the heliospheric modulation region is the reciprocal of G, namely

$$50 \text{ AU}. \qquad (9)$$

V. DISCUSSION

Apart from two regions of low apparent gradient around $\Delta r \approx 2$ and ≈ 8 AU (Figs. 8, 9, and 10), the value of G has been fairly uniform over the range $1 < r < 32$ AU and over a solar cycle variation of intensity by a factor of 2.7 (normalized to same r). This feature of similar data has been exploited by Webber and Lockwood [1981] to yield an estimate of the radius of the heliospheric modulation region ≥ 65 AU. The same authors using data for $E_p > 60$ MeV from Pioneers 10 and 11, Voyagers 1 and 2, and IMP's 7 and 8 find an overall gradient for $1 < r < 23$ AU of +2.85 (± 0.5) percent per AU, significantly but not markedly different than our value of +2.06 (± 0.020). Also Venkatesan et al. [1984a] using independent data from Voyagers 1 and 2 ($E_p > 70$ MeV) and IMP 8 ($E_p > 35$ MeV) find an overall gradient for $1 < r < 13$ AU of 2 to 4 percent per AU and favor a value of +3.5. McKibben et al. [1982] using a still different data set from IMP's 5, 7, and 8 and Pioneers 10 and 11 for $E_p > 67$ MeV find integral radial gradients in the range +1.7 (± 0.6) to +3.9 (± 1.0) percent per AU for various periods of time and various combinations of data from different spacecraft. These authors estimate the radius of the heliosphere as 50 to 70 AU at both solar maximum and solar minimum.

Hence there are mild disagreements among the various groups in measuring essentially the same quantity but a range of 2 to 3 percent per AU for the integral gradient ($E_p > 60$, 80 MeV) now appears to be reliable and is perhaps as accurate as the complex physical situation permits.

McDonald et al. [1981a] using data from Pioneer 10 and Helios 1 and 2, the latter in orbits interior to that of the earth, report a radial gradient out to 22 AU of +3.5 percent per AU in the differential energy range $115 < E_p < 220$ MeV and +3.6 (± 2) to +4.1 (± 2) percent per AU for helium nuclei in the differential specific energy range $114 < \epsilon_\alpha < 380$ MeV/nucleon.

For a threshold $E_p = 80$ MeV and the 1965 (solar minimum) proton and helium spectra of Gloeckler and Jokipii [1967] our integral gradient corresponds to the differential gradient at an effective energy [Van Allen, 1976] in the range 420 to 890 MeV, depending on the energy dependence of the gradient.

Interpretation of a radial gradient usually follows the heliospheric line of thought of Morrison [1956] concerning the 11-year modulation and Forbush decreases of the cosmic ray intensity. In early work, Parker [1956] advocated a geospheric model for both of these effects but later adopted the heliospheric model and led the way in giving it a quantitative structure [Parker, 1963].

In its simplest form the Morrison-Parker model contemplates the emission of ionized magnetized gas from the sun with originally no cosmic rays therein. As the gas (plasma) moves outwards through the solar system, cosmic rays diffuse into the gas clouds which contain "scattering" centers of chaotic magnetic fields. These presumed scattering centers are convected outwards from the sun, tending to carry the population of cosmic rays with them. In a quasi-steady state, the net inward diffusive flux of cosmic rays is taken to be equal to the outward convective flux, viz.

$$D \frac{\partial n}{\partial r} = n v_{sw} \qquad (10)$$

where n is the number density of cosmic rays, D is the macroscopic radial diffusion coefficient, and v_{sw} is the solar wind velocity. Equation (10) ignores factors of the order of unity and other refinements that, though possibly significant, decloud the basic issue and transcend the present state of observational knowledge.

It is further supposed (perhaps incorrectly) that the physical situation is spherically symmetrical and that the modulation region around the sun is spherical with outer radius r_B. The spherical shell bounding this region is called the modulation boundary (for cosmic rays). Inasmuch as it is

impossible for the sun's influence to extend infinitely far, a basic question is the value of r_B. In the spirit of (10), the modulation boundary is coincident with the heliospheric boundary, defined as the spherical shell at which directed flow of the solar wind ceases.

Observationally, passage through the boundary of the heliosphere (a doubtless fluctuating quantity) into the interstellar medium will be easily recognized, viz.:

(a) The cosmic ray intensity will become constant, not subject to solar modulation.

(b) The radial flow of the solar wind will cease.

(c) The solar wind will be replaced by a relatively steady interstellar wind, having a much different velocity vector, temperature, composition, etc.

(d) There will be a substantial transition in the vector magnetic field.

The solar system is in motion relative to a selected set of stars whose proper motions and radial velocities have been measured. From these measurements it is inferred that the velocity vector of the solar system relative to the "local standard of rest" is 19.5 km s^{-1} toward right ascension 271°, declination +30° (the "solar apex") [Abell, 1982] [Allen, 1973]. In ecliptic coordinates the solar apex is at $\lambda = 271°$, $\beta = +53°$.

More recently and of greater significance, the velocity of the solar system relative to the immediately nearby interstellar medium (consisting in part of neutral atomic hydrogen and helium) has been measured. This velocity is ≈ 22 km s^{-1} [Adams and Frisch, 1977] toward right ascension 252°, declination -17°, or toward $\lambda = 254°$, $\beta = +5°$ [Ajello, 1979]. The medium is characterized by $n_H \approx 0.04 - 0.08$ cm^{-3}, $T \approx 10^4$ K, and state of ionization $n_H/n_{H^+} \approx 0.5$ [Paresce, 1984].

These facts have spawned a variety of speculation that the heliospheric boundary may be markedly asymmetric. But because the motion is at a velocity of only 22 km s^{-1} whereas the solar wind velocity is ≈ 440 km s^{-1}, it is not obvious that an asymmetry is significant, especially because the r.m.s. thermal velocity (≈ 16 km s^{-1}) of the atomic hydrogen and the sound velocity in the interstellar medium are comparable to the relative bulk velocity.

It may, nonetheless, be objected that our determination of G by comparing data from P10 with those from P11 is basically faulty because P10 is moving in the upstream direction relative to the interstellar medium whereas P11 is moving in the downstream direction (Figure 1). If the heliosphere is markedly asymmetric along that line, being more extended downstream, then our value of G would be falsely low. Other work, however, comparing both P10 and P11 data out to a common distance of 12 AU with IMP data near the earth [Webber and Lockwood, 1981] gives no evidence for such asymmetry.

The time dependences of the heliographic latitudes of P10 and P11 are shown in Figure 11. In previous work [Van Allen, 1976] on the data for 1975, we found a latitudinal gradient of 0 (± 2) percent per 10° of heliographic latitude. Other recent attempts to determine the latitudinal gradient have been made by Roelof et al. [1983], Decker et al. [1984], and McKibben et al. [1979]. No consensus has yet emerged nor is one likely before high latitude observations by the International Solar Polar Mission in 1986 ff.

For many years, Lockwood [1960] has urged the view that the 11-year solar cycle of cosmic ray intensity is caused by a higher incidence of episodic depressions of the intensity (Forbush decreases) during solar maximum activity from which recovery is sufficiently slow that such overlapping decreases have a cumulative effect. A convincing case for this view is given in Lockwood and Webber [1984]. We are in agreement with this explication as is readily apparent from Figures 2, 3, and 4, and earlier work [Van Allen, 1979]. In Figure 7 we give a detailed presentation of P10, P11, and Deep River Neutron Monitor data for two noteworthy Forbush decreases during 1982. Provisionally, we identify the effects on DOY's 161 at the earth, 187 at P11, and 215 at P10 as attributable to the same change in interplanetary conditions and the effects on

DOY's 195, 219, and 271 as attributable to another. The two episodes are different in detail but both resulted in a durable depression of intensity at both P10 and P11 [cf. Van Allen, 1979]. The details of the two cases are given in Table 1.

From the definition of G and equation (10),

$$G = \frac{1}{n}\frac{\partial n}{\partial r} = \frac{v_{sw}}{D} \quad . \tag{11}$$

Using observed values of G, 0.02 $(AU)^{-1}$, and v_{sw}, 440 km s^{-1},

$$D = 3.3 \times 10^{22} \text{ cm}^2 \text{ s}^{-1} = 4600 \text{ (AU)}^2 \text{ yr}^{-1}. \tag{12}$$

The corresponding scattering mean-free-path,

$$= \frac{3D}{c} = 3.3 \times 10^{12} \text{ cm} = 0.22 \text{ AU}. \tag{13}$$

This value of the mean-free-path may be compared to the gyro-radius of a proton of, say, 2 GeV energy in an interplanetary magnetic field of 5×10^{-5} gauss, namely 0.06 AU.

The above calculations are intended only to fix the orders of magnitude of quantities and make no pretense to accuracy (e.g., D may be a function of r, t, and particle energy).

We now have a direct measurement that $r_B > 32$ AU and a reliable estimate of the scale length of the modulation region, namely 50 AU. Nonetheless, r_B may well be considerably greater than 50 AU.

One simple method of estimating r_B is to suppose that the boundary of the heliosphere is at the radial distance at which the dynamic pressure of the solar wind equals the interstellar magnetic field pressure $B^2/8\pi$, namely,

$$n m v_{sw}^2 \approx B^2/8\pi \ . \qquad (14)$$

Taking $n = 5/r^2$, $v_{sw} = 440$ km s^{-1}, $m = 1.67 \times 10^{-24}$ g, and $B = 7 \times 10^{-6}$ gauss [Allen, 1973], one finds from (14) that $r_B \approx 90$ AU. But the uncertainties in the various quantities do not permit much confidence in the result nor do they permit much confidence in claiming a variation of r_B with solar activity.

Another method of estimating r_B is to use modulation theory, such as it is, to "demodulate" the spectrum to interstellar space and then to estimate, using observed values of the differential gradient g, the value of r at which the demodulated spectrum would occur. By this means McKibben et al. [1982] estimate that r_B is 50 to 70 AU, at both solar maximum and solar minimum.

We have noted above that Webber and Lockwood [1981] have used a kindred method to estimate that $r_B > 65$ AU.

Still another method of estimating r_B is to suppose that the volume density of cosmic ray kinetic energy in interstellary space is equal to $B^2/8\pi$ therein. Such an "equipartition" of energy is discussed critically by Cowling [1967], who gives some support to that concept but also expresses doubt as to its validity. Nonetheless it yields results of some interest. Using the proton and helium spectra of Gloeckler and Jokipii [1967], we calculate the volume density $\mathcal{e}$ of galactic cosmic rays at 1 AU at solar minimum by numerical integration of the following

$$\mathcal{e} = \frac{4\pi}{c} \int_{80}^{\infty} \frac{E}{\beta} \frac{dj}{dE} \, dE \qquad (15)$$

wherein β is the ratio of the speed of the particle to the speed of light c and dj/dE is the differential unidirectional spectral intensity. The results are

$$\mathcal{e}_p = 7.3 \times 10^{-13} \text{ erg cm}^{-3}$$

(about 16% of which is for particle energies below 2000 MeV, the modulation sensitive energy region)

and $$\mathcal{e}_\alpha = 3.2 \times 10^{-13} \text{ erg cm}^{-3}$$

(about 19% of which is below 2000 MeV/nucleon). The sum

$$\mathcal{E} = \mathcal{E}_p + \mathcal{E}_\alpha = 1.0 \times 10^{-12} \text{ erg cm}^{-3}. \qquad (16)$$

For an interstellar magnetic field $B = 7 \times 10^{-6}$ gauss [Allen 1973]

$$\frac{B^2}{8\pi} = 1.9 \times 10^{-12} \text{ erg cm}^{-3} . \qquad (17)$$

Thus it appears possible for the modulation-sensitive portion of the spectrum to increase by a factor of $\approx e^2$ above its 1 AU value in order to approximate quasi-equipartition in the interstellar medium. This line of thought suggests that $r_B \approx (2)(50) = 100$ AU.

Finally, it appears possible to base an estimate of r_B on the 1 year lag in response of the cosmic ray intensity, even at ≈ 30 AU, to solar activity as measured by sunspot numbers (Figure 6) [cf. Fulks, 1975]. A grossly simplified model for this effect is along the following lines. First suppose that a steady state has been established with a particular value of D throughout the heliosphere. Then suppose that the conditions at the sun change suddenly so that D increases by, say, a factor of 2. The spherical region of higher D expands outward at velocity v_{sw} until it reaches the heliospheric boundary, wherever that

may be. The time constant τ for the increase of intensity interior to the expanding region is of the order of

$$\tau \approx 0.5 \frac{r_B^2}{D} . \tag{18}$$

Hence

$$r_B \approx \sqrt{\frac{D\tau}{0.5}} \tag{19}$$

wherein $D \approx 4600\ (AU)^2\ yr^{-1}$ and $\tau \approx 1$ yr. By (19),

$$r_B \approx 100\ AU .$$

In one year, the solar wind travels ≈ 93 AU, giving some plausibility to this result.

None of the foregoing estimates of r_B withstands critical scrutiny but they do give some feeling for the nature of the problem.

Observationally, $r_B > 32$ AU and it would not be astonishing if its value lies between 50 and 100 AU. The value of r_B may systematically decrease during solar minimum conditions and increase during solar maximum conditions and may moreover undergo sporadic fluctuations of many AU as the dynamic pressure of the

solar wind fluctuates. Observations during the next decade should yield an improved estimate of r_B or perhaps an actual determination.

APPENDIX I. Remarks on Validity and Accuracy of Data

1. Individual counting rates of a number of miniature Geiger-Mueller tubes provide the basic data for the present paper. These GM tubes were built by the EON Corporation. All of them are halogen-quenched, "infinite lifetime" tubes. Detectors A, B, C, and G on Pioneer 10 (Van Allen et al., 1974) and A, B, and C on Pioneer 11 (Van Allen et al., 1980) are EON Type 6213. Similar tubes have been used previously in University of Iowa instruments on Explorer 4, Pioneer 3, Pioneer 4, Explorer 7, Injun 1, Explorer 12, TRAAC, Mariner 2, Explorer 14, Explorer 15, Injun 3, OGO 1, Injun 4, Mariner 4, OGO 2, Explorer 33, Mariner 5, Explorer 35, Injun 5, and Hawkeye 1. Tubes in those instruments logged over 700,000 detector-hours of reliable operation in flight. Many individual tubes experienced over 10^{10} counts and a few, over 10^{11} counts.

Detectors D, E, and F on each spacecraft are EON Type 5107, being of different size and shape than the 6213's as described in detail in the second of the foregoing references. Tubes of this type had not been flown before but were found, after selection and testing, to have excellent reliability.

The tubes that were assembled in the flight units were the survivors of a rigorous selection procedure on a large batch of each of the two types of tube. The procedure involved mechanical vibration testing and then running the plateau curves (counting rate vs. applied voltage when exposed to a fixed γ-ray source) as a function of temperature and of exposure age. Of the order of 10^8 counts were accumulated on each tube. About 10% of the tubes were judged suitable for flight. The selected tubes were assembled in flight units and again subjected to $\sim 10^8$ counts by hard x-ray and Co^{60} sources for the determination of apparent vs. true counting rate curves before and after an extended program of thermal-vacuum testing. Each of the completed instruments including detectors operated properly over the temperature range -20° to +100° F. The temperature coefficient of counting rate for a fixed Co^{60} γ-ray source was determined for each tube (and its associated circuitry) as assembled in the flight unit over the temperature range -20° to +90° F. For Pioneer 10, the mean coefficient was 3.98×10^{-4} per degree Fahrenheit for A, B, C, and G and -2.18×10^{-4} per degree Fahrenheit for D, E, and F. For Pioneer 11, the mean coefficient was 3.69×10^{-4} per degree Fahrenheit for A, B, and C and -6.5×10^{-4} for D, E, and F.

All observed flight rates are corrected to +75° F using the above coefficients and the measured temperature of the detector assembly (see next paragraph).

The in-flight temperature of a calibrated thermistor imbedded in our detector assembly is telemetered continuously. For both Pioneer 10 and Pioneer 11, the highest temperature (+77° F) occurred on the day of launch. The temperature declined rapidly to about 48° F during the first two months and then more slowly to +40° F (P 10) and +45° F (P 11) by the end of the first year of flight. Thereafter the temperatures have declined linearly with time at the rate of 2° F per year. As of April 1984, both temperatures were +20.6° F (following turn-off of power to the IPP instrument on Pioneer 11). These temperatures, essentially independent of the intensity of sunlight for the past ten years, are dependent principally on the power dissipated in the instrument (0.72 watt) and in other instruments on the instrument platform of the spacecraft. We anticipate no problem with temperature during the prospective lifetime of either spacecraft. Power sharing (i.e., alternate on-off operation) among the instruments on Pioneer 11 will be initiated in late 1984, and on Pioneer 10 about two years later. This procedure will lower the "power-off" temperature of our detector assembly by $\leq 8°$ F.

Because of the gradual and small change of the temperatures during most of the duration of the two missions and of the small magnitude of the temperature coefficients, the estimated uncertainties in the adopted values of the coefficients have a trivial effect on the results of the present study.

3. The spacecraft bus voltage is regulated at 28.0 V (± 1%) and the terminal voltage of the internal power supply for the electronics in our instrument is separately regulated at +7.92 V (± 2%). Both of these voltages are telemetered continuously via an analog-to-digital converter having 64 linear steps. Both voltages on both spacecraft have been invariant throughout their flight periods. A change of one digital step would be a matter of some concern but our instrument is unaffected by a change in bus voltage over the range 26 to 29 V.

4. No one of the GM tubes has exhibited any anomaly (i.e., spuriously high or low counting rates or failure to count) at any time before or since launch (now over twelve years of flight for Pioneer 10, including passage through the outer and inner radiation belts of Jupiter, and over eleven years of flight for Pioneer 11, including passage through the outer and inner radiation belts of both Jupiter and Saturn). Each of the least shielded GM tubes (Detector A) has experienced about 3×10^{10} counts during the missions to date and the more heavily shielded tubes, about an order of magnitude fewer counts. The dominant contribution occurred during passage through Jupiter's magnetosphere in both cases. No discontinuous change in interplanetary counting rates of any detector before and after the encounters was observed.

Inasmuch as it was not feasible to provide an in-flight radiation source for an end-to-end check of the GM tubes and their associated electronics, there is no direct basis for ruling out gradual drifts in sensitivity. There are, however, four grounds for considering drifts unlikely:

(a) Extensive laboratory experience;

(b) The likelihood that any such drift would be characteristic of an individual tube.

(c) The accurate constancy of the ratios of the interplanetary counting rates among the several tubes on the same spacecraft, e.g., D_{10}/C_{10}, etc. throughout the missions; and

(d) The close agreement of the time-variability of the three independent ratios of the counting rates of corresponding tubes on the separate spacecraft, B_{10}/B_{11}, C_{10}/C_{11}, and D_{10}/D_{11} (see text).

Points (c) and (d) support (b) by the additional fact that, as noted above, Detectors D are of a quite different type than are Detectors B and C.

5. Detector A on Pioneer 11 has no shielding over its thin mica-window and is sensitive to low energy particles; it detects numerous solar and interplanetary particle events so that its rate is seldom at the cosmic ray background level. Also, Detector G on Pioneer 10 is a GM tube but such a tube was replaced by a solid state detector on Pioneer 11. Hence,

in the present study we have settled on study of the three ratios B_{10}/B_{11}, C_{10}/C_{11}, and D_{10}/D_{11}. The correspondingly designated detectors on the two spacecraft have virtually identical shielding and physical placement in the instrument package. However, we find that virtually the same results are obtained using ratios such as C_{10}/B_{11}, etc.

6. The concordant results (see text) among the three adopted counting rate ratios provide overall confidence in the validity of the observational data, irrespective of detailed considerations.

7. On the basis of theoretical failure analysis, two independent signal processors (for converting the GM pulses to a quasi-logarithmically-scaled digital output) were included in each instrument. During Pioneer 11's encounter with Jupiter in December 1974, a failure (presumably attributable to cumulative radiation damage) occurred in high order bits of one of the two channels of the "standby" processor. By radio command, this processor was replaced by the "main" processor. The latter has functioned properly throughout the subsequent flight. No anomaly of any kind at any time has occurred in either of the two processors on Pioneer 10.

8. The electrical power for each of the two spacecraft is provided by four Type SNAP 19 Radioisotope Thermal Generators (RTG's) of the Atomic Energy Commission. The heating of the thermoelectric system is provided by a mixture of plutonium

isotopes, the most important of which is Pu^{238} (half life 86.4 years). The total activity of Pu^{238} in the four units is 77,000 curies (2500 watts thermal). There are several much weaker Radioisotope Heater Units (RHU's), also using plutonium, for spot heating. The typical isotopic composition by weight [Kaminskas et al., 1971] of the plutonium "fuel" by nuclear mass number is 238, 80%; 239, 15.8%; 240, 2.8%; 241, 1%; 242, 0.4%; and 236, 1 part per million. Basic data on half-lives, decay schemes, etc. are known for all of these isotopes. Using these data, extensive overall data on the RTG's, and laboratory tests on our apparatus, we have concluded that Pu^{236}, despite its low relative abundance, is the dominant constituent in causing increasing background counting rates of our GM detectors as a function of time following fuel separation. The next most important contribution (declining with time) to the background rates comes from L x-rays of energy ~ 100 keV from U^{234}, the long-lived daughter of the alpha particle decay of Pu^{238}.

The complex decay chain of Pu^{236} (half-life 2.85 years) and the emissions from successive progeny have been described and discussed by Kaminskas et al. [1971], Thomsen [1974], and Thomsen and Van Allen [1976] and have been reviewed recently by the current authors. The principal conclusion is that the abundance of Tl^{208} in the Pu^{236} decay chain is, following a year or two of aging, the most important measure of counting rate

background by virtue of the 2.61 MeV γ-ray from an excited state of its stable daughter Pb^{208}. The abundance of Tl^{208} is, in turn, proportional, at any given time, to the abundance of one of its ancestors Th^{228}. The latter increases from essentially zero at the time of fuel separation to a maximum value 18.6 years later and then declines gradually.

Prelaunch tests with the flight RTG's and our flight instrument on the spacecraft were made in the assembly room of TRW Systems, Inc. for the purpose of determining the background counting rates of all GM tubes. Also, simulated aging tests were done by adding Th^{228} sources of calculated activity during these tests. In our earlier work [Van Allen, 1972; Thomsen, 1974; Thomsen and Van Allen, 1976; Van Allen, 1979, 1980] on the cosmic ray gradient, a theoretical curve of the activity of Th^{228} as a function of time was fit to these test data and, despite some mild internal inconsistencies, this curve was used to calculate the subtractive corrections to all observed counting rates.

9. During the Saturn encounter of Pioneer 11 there occurred a unique and precious opportunity to check the magnitude of the RTG corrections under free space conditions. The spacecraft passed under the dense Rings A and B of Saturn into periapsis at 1.24 R_s. The mean counting rates of GM tubes A, B, and C are plotted as a function of radial distance in Figure 12. After correction for the contribution of primary cosmic rays

(using Stø rmer cut-off theory) and of secondaries produced in the rings after the fashion of Chenette et al. [1980], we find the residual mean counting rate of A, B, and C to be $\bar{R}_{11} = 0.272 \pm 0.010$ c s^{-1} (Figure 12). This rate is assigned solely to the RTG's.

Using our previous formulae based on preflight tests a rate of 0.50 c s^{-1} was calculated for this time. This important discrepancy is not really understood but is thought attributable to room scattering during the preflight tests and uncertainties in the simulated aging tests. We now believe that the previously published strong upturn in the radial dependence of C_{10}/C_{11}, etc. following the major Forbush decrease of cosmic ray intensity in April-May 1978 is spurious, having been caused by the excessively large RTG corrections as applied to the then much reduced rates. [See Figure 4 (a), (b), and (c) of Van Allen, 1980.] Previous to that time the ratios were much less affected by the excessive correction.

We have adopted the Saturn encounter value of $\bar{R}_{11}$ and believe it to be reliable to ± 5%. The corrections for individual detectors A, B, C, and D are derived from the mean value in accordance with the ratios of their interplanetary counting rates during quiet conditions, viz.:

$$R\,(A_{11}) = 1.137\,\bar{R}_{11}$$
$$R\,(B_{11}) = 0.905\,\bar{R}_{11}$$
$$R\,(C_{11}) = 0.958\,\bar{R}_{11}$$
$$R\,(D_{11}) = 0.254\,\bar{R}_{11}$$

Our working formula for calculating the time dependence of the mean subtractive correction $\bar{R}_{11}$ is based on AEC supplied information on the isotopic composition of the several RTG's, dates of separation of the fuel, etc., and on basic radioactive decay-chain data (cf. Thomsen and Van Allen, 1976). The correction curve was fit to the Saturn-encounter point and to the preflight point (as adjusted downward for estimated room scattering). The curve is principally dependent on the former, well-determined point and only weakly dependent on the re-estimated preflight point. Our adopted algebraic formula is

$$\bar{R}_{11} = 1.103 \times 10^{-2} [2\,f(t) + 0.9\,f\,(t + 0.832)] + 5.53 \times 10^{-3} [3\,g(t) + g\,(t + 0.832)] \quad c\,s^{-1}$$

where

$$f\,(t) = 23.792 \exp(-0.3623\,t) + 12.120 \exp(-0.0094\,t) - 35.912 \exp(-0.2432\,t),$$

$$g\,(t) = \exp(-0.0081\,t),$$

and t is measured in years with t = 0 on 15 March 1971 (DOY 74). A plot of $\bar{R}_{11}$ vs. time is given in Figure 13.

There is no corresponding determination of the in-flight, free-space value of the RTG corrections for Pioneer 10. Hence we have assumed that they can be derived from the corrections for Pioneer 11, using the somewhat different values of isotropic composition of the plutonium, dates of separation, etc. Our adopted algebraic formula is

$$\bar{R}_{10} = 3.862 \times 10^{-2} f(t) + 2.211 \times 10^{-2} g(t) \quad c\ s^{-1}$$

where f(t) and g(t) are as previously specified and t is the time in years with t = 0 on 15 June 1970 (DOY 166). A plot of $\bar{R}_{10}$ vs. time is also given in Figure 13.

$$R\ (A_{10}) = 1.085\ \bar{R}_{10}$$
$$R\ (B_{10}) = 0.903\ \bar{R}_{10}$$
$$R\ (C_{10}) = 1.012\ \bar{R}_{10}$$
$$R\ (D_{10}) = 0.309\ \bar{R}_{10}$$
$$R\ (G_{10}) = 0.903\ \bar{R}_{10}$$

10. The duty cycle for accumulating counts from each of the GM tubes A, B, C, and D is 1/11, irrespective of telemetry bit rate. Thus, in a solid 24 hours of telemetry reception at a typical counting rate (for A, B, or C) of 0.8 c s^{-1}, 6300 counts are recorded. The statistical standard deviation of such a one-day

mean is 1.3% or of a 25-day mean, 0.3%. The actual telemetry reception approached 100% early in the missions but later has been more typically in the range 8 to 16 hours per day with a corresponding increase in relative statistical standard deviation. The typical counting rate of the GM tubes D is about 0.3 c s^{-1} and the statistical standard deviation is larger than those computed above by a factor of 1.6.

The r.m.s. fluctuation of mean daily rates from the mean rate for a 25-day period is never less than several times as great as the statistical expectation -- presumably signifying real physical fluctuations.

Acknowledgments

This work has been supported by Ames Research Center/NASA contract NAS2-11125, Office of Naval Research Contract N00014-76-C-0016, and NASA Headquarters Grant NGL-16-001-002. We are especially indebted to Mr. R. O. Fimmel et al. at the Ames Research Center for maintaining Pioneer 10/11 operations and data reception.

REFERENCES

Abell, G. O., Exploration of the Universe, 4th Ed., Saunders College Publishing, Philadelphia, 1982.

Adams, T. F., and P. C. Frisch, High resolution observations of the Lyman alpha sky background, Astrophys. J., 212, 300-308, 1977.

Ajello, J. M., An interpretation of Mariner 10 helium (584 Å) and hydrogen (1216 Å) interplanetary emission observations, Astrophys. J., 222, 1068-1079, 1979.

Allen, C. W., Astrophysical Quantities, 3rd Ed., University of London, The Athlone Press, 1973.

Chenette, D. L., J. F. Cooper, J. H. Eraker, K. R. Pyle, and J. A. Simpson, High-energy trapped radiation penetrating the rings of Saturn, J. Geophys. Res., 85, 5785-5792, 1980.

Cowling, T. G., Interstellar and interplanetary plasmas, Quarterly J. Royal Astron. Soc., 8, 130-141, 1967.

Decker, R. B., S. M. Krimigis, and D. Venkatesan, Estimate of cosmic-ray latitudinal gradient in 1981-1982, Astrophys. J., 278, L119-L122, 1984.

Fulks, G. J., Solar modulation of galactic cosmic ray electrons, protons, and alphas, J. Geophys. Res., 80, 1701-1714, 1975.

Gloeckler, G., and J. R. Jokipii, Solar modulation and the energy density of galactic cosmic rays, Astrophys. J., 148, L41-L46, 1967.

Kaminskas, R. A., J. S. Brunhouse, and K. T. Hartwig, RTG/Science instrument radiation interactions for deep space probes, Phase II, III and IV, TRW Systems Group, Redondo Beach, CA 90278, January 1971.

Lockwood, J. A., On the long-term variation in the cosmic radiation, J. Geophys. Res., 65, 19-25, 1960.

Lockwood, J. A., and W. R. Webber, Observations of the dynamics of the cosmic ray modulation, J. Geophys. Res., 89, 17-25, 1984.

McDonald, F. B., N. Lal, J. H. Trainor, M. A. I. Van Hollebeke, and W. R. Webber, The solar modulation of galactic cosmic rays in the outer heliosphere, Astrophys. J., 249, L71-L75, 1981a.

McDonald, F. B., J. H. Trainor, J. D. Mihalov, J. H. Wolfe, and W. R. Webber, Radially propagating shock waves in the outer heliosphere: the evidence from Pioneer 10 energetic particle and plasma observations, Astrophys. J., 246, L165-L169, 1981b.

McKibben, R. B., K. R. Pyle, and J. A. Simpson, The solar latitude and radial dependence of the anomalous cosmic-ray helium component, Astrophys. J., 227, L147-L152, 1979.

McKibben, R. B., K. R. Pyle, and J. A. Simpson, The galactic cosmic-ray radial intensity gradient and large-scale modulation in the heliosphere, Astrophys. J., 254, L23-L27, 1982.

Morrison, P., Solar origin of cosmic-ray time variations, Phys. Rev., 101, 1397-1404, 1956.

Paresce, F., On the distribution of interstellar matter around the sun, Astron. J., 89, 1022-1037, 1984.

Parker, E. N., Modulation of primary cosmic-ray intensity, Phys. Rev., 103, 1518-1533, 1956.

Parker, E. N., Interplanetary Dynamical Processes, Interscience Publishers, New York, 1963.

Roelof, E. C., R. B. Decker, and S. M. Krimigis, Latitudinal and field-aligned cosmic ray gradients 2 to 5 AU: Voyagers 1 and 2 and IMP 8, J. Geophys. Res., 88, 9889-9909, 1983.

Solar-Geophysical Data, Environmental Data and Information Service, National Oceanic and Atmospheric Administration, Boulder, Colorado, monthly issues, 1972-1974.

Thomsen, M. F., The heliocentric radial cosmic ray gradient, M.S. thesis, University of Iowa, 1974.

Thomsen, M. F., and J. A. Van Allen, Galactic cosmic-ray intensity 0.99 to 5.26 astronomical units from the sun, Astrophys. J., 206, 599-615, 1976.

Van Allen, J. A., Observations of galactic cosmic-ray intensity at heliocentric radial distances from 1.0 to 2.0 astronomical units, Astrophys. J., 177, L49-L52, 1972.

Van Allen, J. A., Galactic cosmic ray intensity from 1 to 9 AU, Geophys. Res. Lett., 3, 425-428, 1976.

Van Allen, J. A., Propagation of a Forbush decrease in cosmic ray intensity to 15.9 AU, Geophys. Res. Lett., 6, 566-568, 1979.

Van Allen, J. A., Galactic cosmic-ray intensity to a heliocentric distance of 18 AU, Astrophys. J., 238, 763-767, 1980.

Van Allen, J. A., D. N. Baker, B. A. Randall, and D. D. Sentman, The magnetosphere of Jupiter as observed with Pioneer 10: 1, instrument and principal findings, J. Geophys. Res., 79, 3559-3577, 1974.

Van Allen, J. A., B. A. Randall, and M. F. Thomsen, Sources and sinks of energetic electrons and protons in Saturn's magnetosphere, J. Geophys. Res., 85, 5679-5694, 1980.

Venkatesan, D., R. B. Decker, and S. M. Krimigis, Radial gradient of cosmic ray intensity from a comparative study of data from Voyager 1 and 2 and IMP 8, J. Geophys. Res., 89, 3735-3746, 1984a.

Venkatesan, D., R. B. Decker, S. M. Krimigis, and J. A. Van Allen, The galactic cosmic ray intensity minimum in the inner and outer heliosphere in solar cycle 21, J. Geophys. Res. (submitted), 1984b.

Webber, W. R., and J. A. Lockwood, A study of the long-term variation and radial gradient of cosmic rays out to 23 AU, J. Geophys. Res., 86, 11,458-11,462, 1981.

Table 1

Data on Two Large Forbush Decreases
(Fig. 7)

	1982 DOY	% Decrease	r AU	λ
First Event				
Deep River Neutron Monitor	161 ± 1	10	1.02	258°8
Pioneer 11	187 ± 2	18	12.1	220.3
Pioneer 10	215 ± 1	14	27.9	65.5
Second Event				
Deep River Neutron Monitor	195 ± 1	21	1.02	291.2
Pioneer 11	219 ± 1	21	12.3	221.5
Pioneer 10	271 ± 1	16	28.3	65.7

Notes:

(1) The two events are qualitatively different in nature.

(2) The apparent velocities of propagation $\Delta r/\Delta t$ (ignoring differences in longitude) for the first event are 740 ± 60 km s^{-1} from the earth to P11 and 860 ± 30 km s^{-1} from the earth to P10.

(3) The apparent velocities of propagation for the second event are 810 ± 50 km s^{-1} from the earth to P11 and 620 ± 15 km s^{-1} from the earth to P10. The discrepancy in apparent velocities in this case is presumed to be due to the more directional nature of the second event, as evidenced by the neutron monitor curve, and the neglect of corotation time to reach P10.

CAPTIONS FOR FIGURES

Fig. 1. Ecliptic plane projection of the trajectories of Pioneer 10, Pioneer 11, Voyager 1, and Voyager 2. Also shown are the orbit of the earth and portions of the orbits of Jupiter, Saturn, and Uranus; and a table of dates of launch and closest approach of the four spacecraft to Jupiter, Saturn, and Uranus. The X-axis points to the earth's vernal equinox ($\lambda = 0°$ at this point and increases counterclockwise).

Fig. 2. Fully corrected daily mean counting rates of GM detectors B on Pioneers 10 and 11 as a function of time. Heliocentric radial distances are given by the upper scale for Pioneer 11 and the lower scale for Pioneer 10.

Fig. 3. Same as Figure 2, except for GM detectors C.

Fig. 4. Same as Figure 2, except for GM detectors D.

Fig. 5. A repeat of Fig. 3 with the addition of the daily mean counting rate (of the Deep River Neutron, Lat 46°10 N, Long 282°50 E, alt 145 m). The ordinate is in counts $hr^{-1}/300$ [Solar-Geophysical Data, 1972-1984].

Fig. 6. Comparison plots of the counting rates of GM detector C on Pioneer 10 and monthly mean sunspot numbers [Solar-Geophysical Data, 1972-74]. Note that the latter plot is inverted. A portion at the right hand end of the sunspot number plot has been moved to the right by 1.1 year and superimposed on the cosmic ray intensity plot in the upper panel to illustrate the time delay.

Fig. 7. Graphical comparison of the data from Pioneer 10 and Pioneer 11 with those from the Deep River Neutron Monitor for two large Forbush decreases in mid-1982.

Fig. 8. Semilogarithmic plot of the "delayed" ratios of twenty-five-day mean counting rates of GM detectors B on Pioneer 10 and on Pioneer 11 vs. Δr, the difference in the heliocentric radii. The straight line is the least-squares fit to the data of an equation of the form $\exp(G\,\Delta r)$.

Fig. 9. Same as Figure 8, except for GM detectors C.

Fig. 10. Same as Figure 8, except for GM detectors D.

Fig. 11. Heliographic latitudes of Pioneer 10 and Pioneer 11 vs. time.

Fig. 12. Mean counting rates of GM detectors A, B, and C on Pioneer 11 vs. radial distance from the center of Saturn during the 1 September 1979 encounter.

Fig. 13. Adopted curves of the time dependence of the mean RTG corrections to the counting rates of GM detectors A, B, and C on Pioneer 10 and Pioneer 11. The corrections are subtracted from the raw counting rates after temperature correction of the latter.

D-G80-551-2

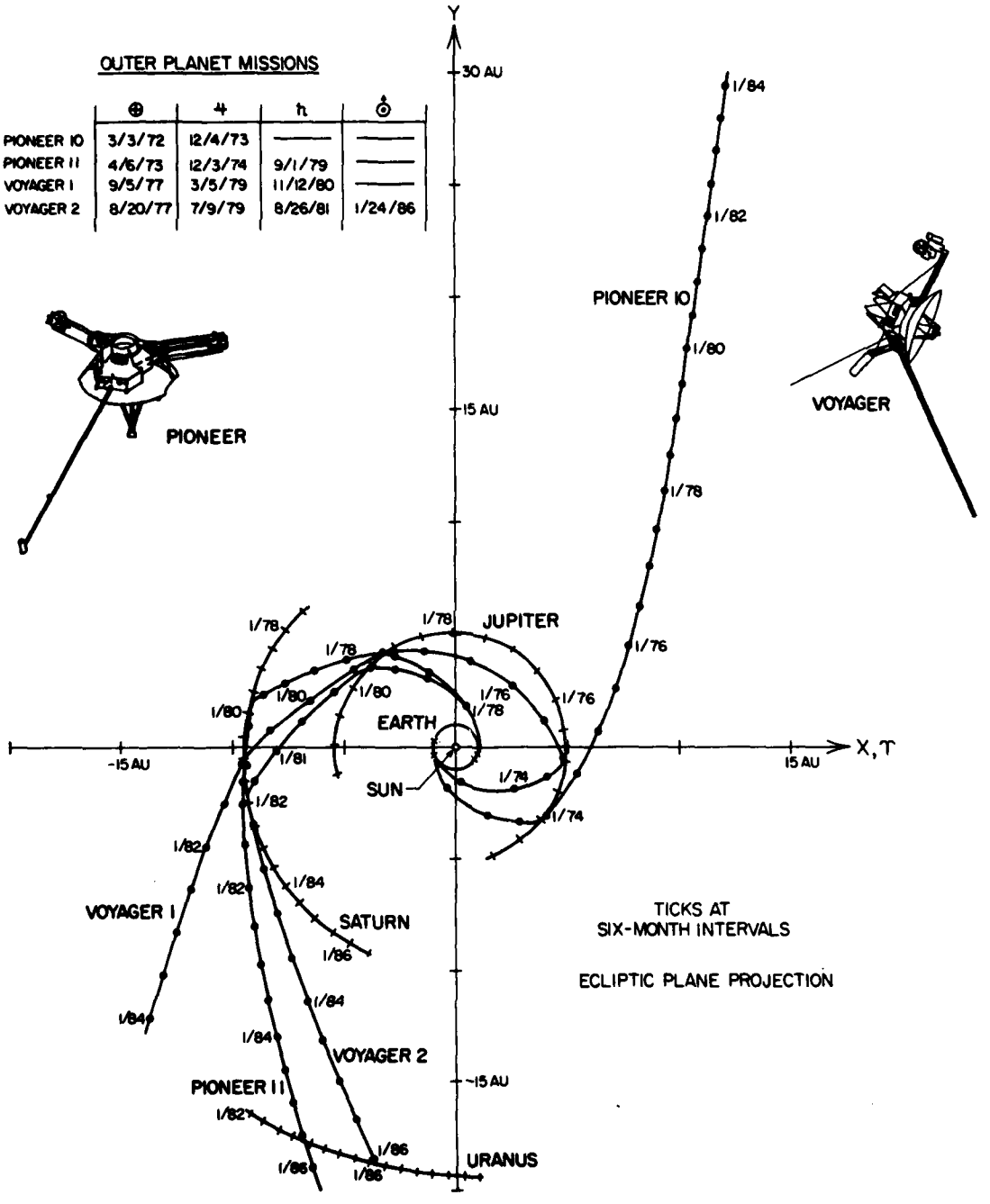

Figure 1

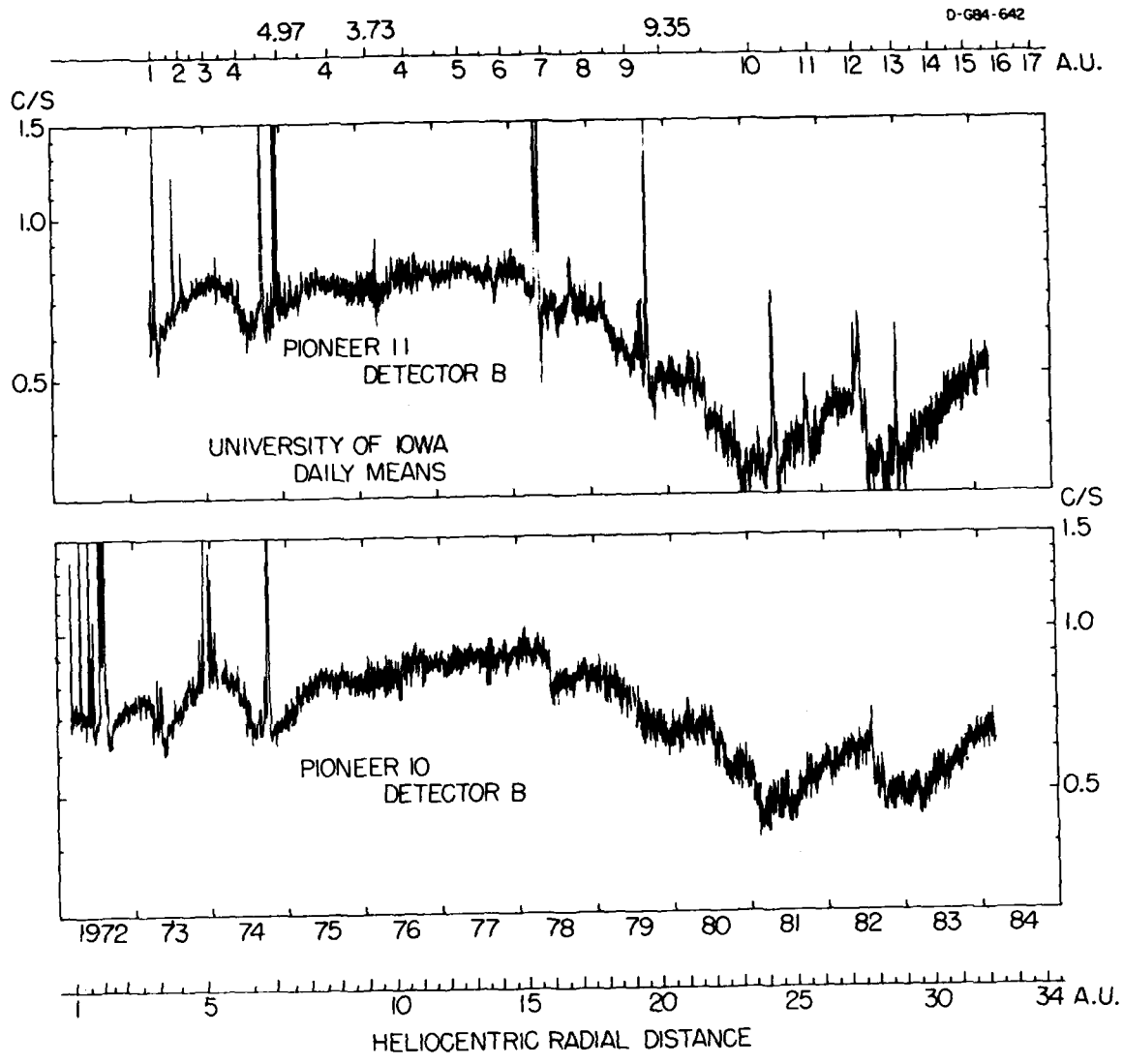
D-G84-642
4.97
3.73
9.35
1 2 3 4 4 4 5 6 7 8 9 10 11 12 13 14 15 16 17 A.U.
C/S
1.5
1.0
0.5
PIONEER 11
DETECTOR B
UNIVERSITY OF IOWA
DAILY MEANS
C/S
1.5
1.0
0.5
PIONEER 10
DETECTOR B
1972 73 74 75 76 77 78 79 80 81 82 83 84
1 5 10 15 20 25 30 34 A.U.
HELIOCENTRIC RADIAL DISTANCE

Figure 2

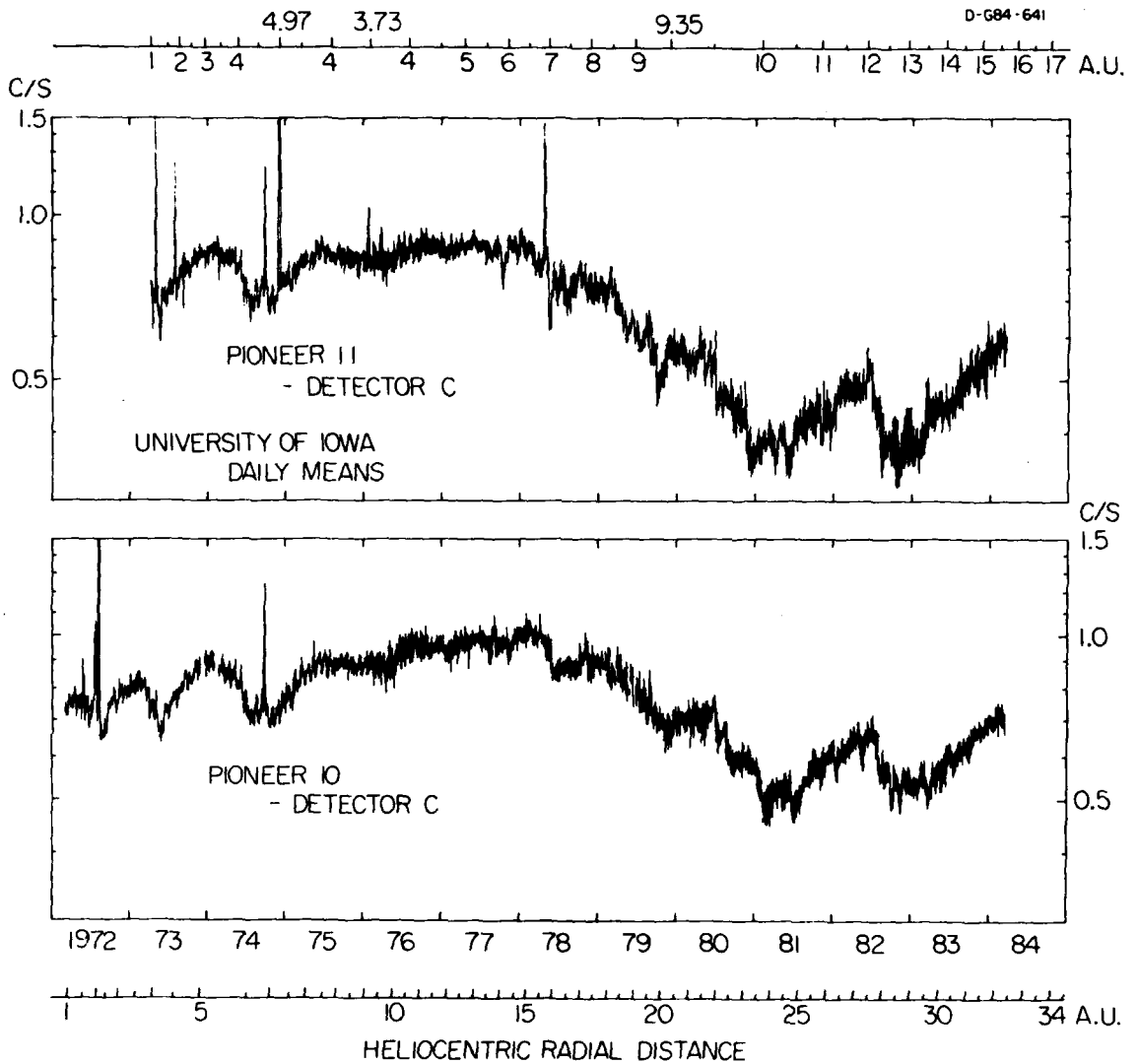
4.97
3.73
9.35
D-G84-641
1 2 3 4 4 4 5 6 7 8 9 10 11 12 13 14 15 16 17 A.U.
C/S
1.5
1.0
0.5
PIONEER 11
- DETECTOR C
UNIVERSITY OF IOWA
DAILY MEANS
C/S
1.5
1.0
0.5
PIONEER 10
- DETECTOR C
1972 73 74 75 76 77 78 79 80 81 82 83 84
1 5 10 15 20 25 30 34 A.U.
HELIOCENTRIC RADIAL DISTANCE

Figure 3

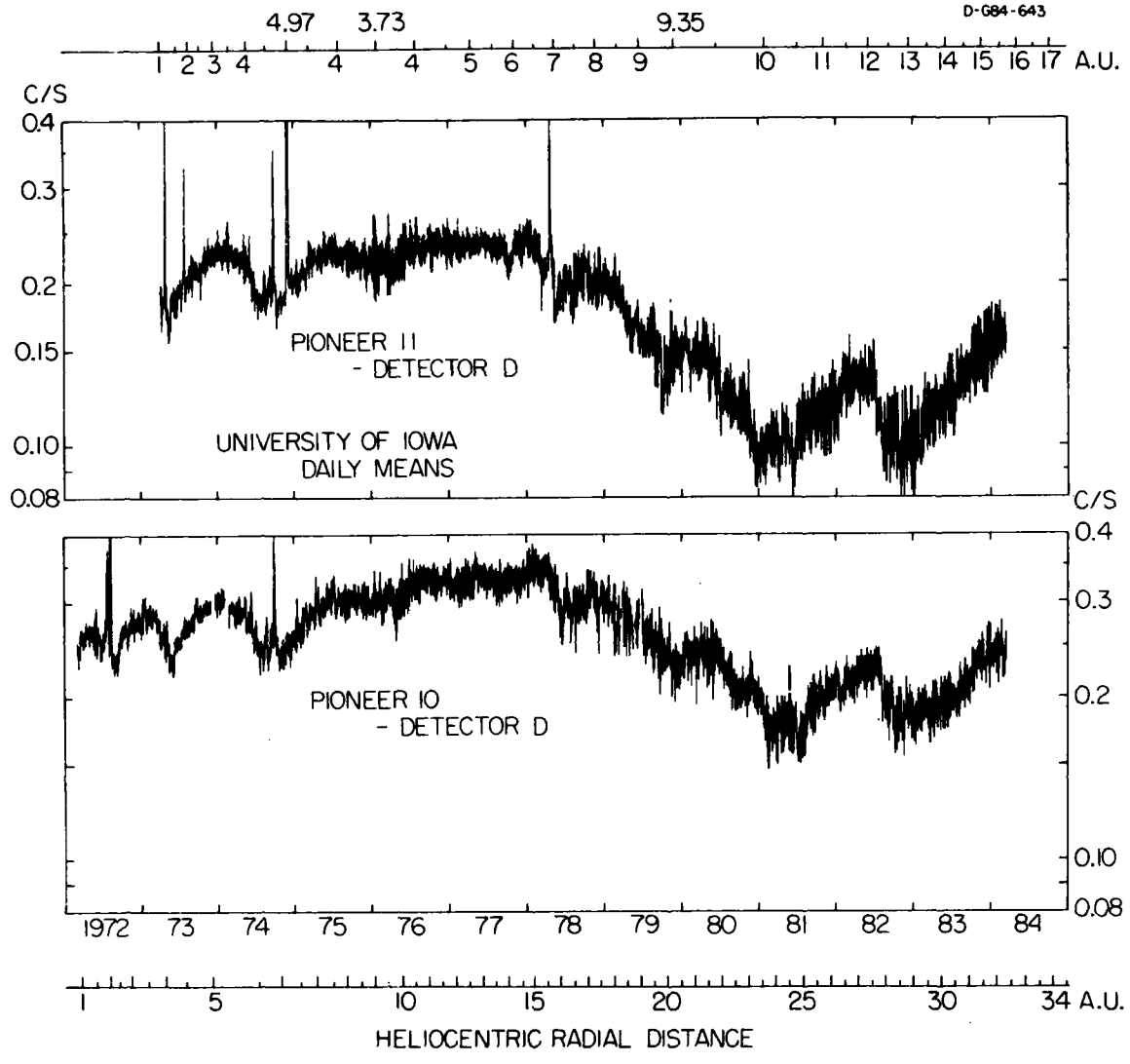
D-G84-643
4.97
3.73
9.35
1 2 3 4 4 4 5 6 7 8 9 10 11 12 13 14 15 16 17 A.U.
C/S
0.4
0.3
0.2
0.15
0.10
0.08
PIONEER 11
- DETECTOR D
UNIVERSITY OF IOWA
DAILY MEANS
C/S
0.4
0.3
0.2
0.10
0.08
PIONEER 10
- DETECTOR D
1972 73 74 75 76 77 78 79 80 81 82 83 84
1 5 10 15 20 25 30 34 A.U.
HELIOCENTRIC RADIAL DISTANCE

Figure 4

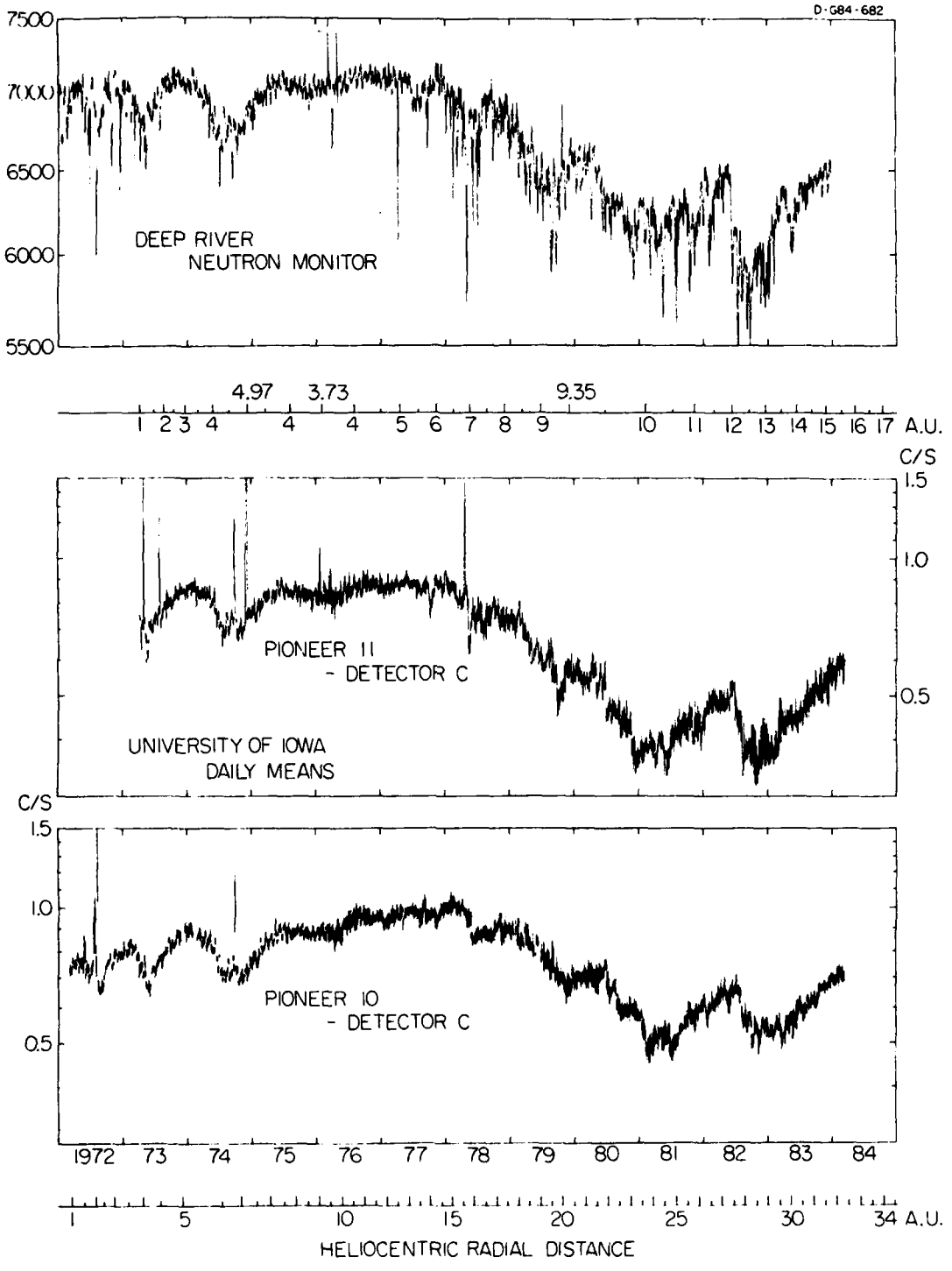
D-G84-682
7500
7000
6500
6000
5500
DEEP RIVER
NEUTRON MONITOR
4.97
3.73
9.35
1 2 3 4 4 4 5 6 7 8 9 10 11 12 13 14 15 16 17 A.U.
C/S
1.5
1.0
0.5
PIONEER 11
- DETECTOR C
UNIVERSITY OF IOWA
DAILY MEANS
C/S
1.5
1.0
0.5
PIONEER 10
- DETECTOR C
1972 73 74 75 76 77 78 79 80 81 82 83 84
1 5 10 15 20 25 30 34 A.U.
HELIOCENTRIC RADIAL DISTANCE

Figure 5

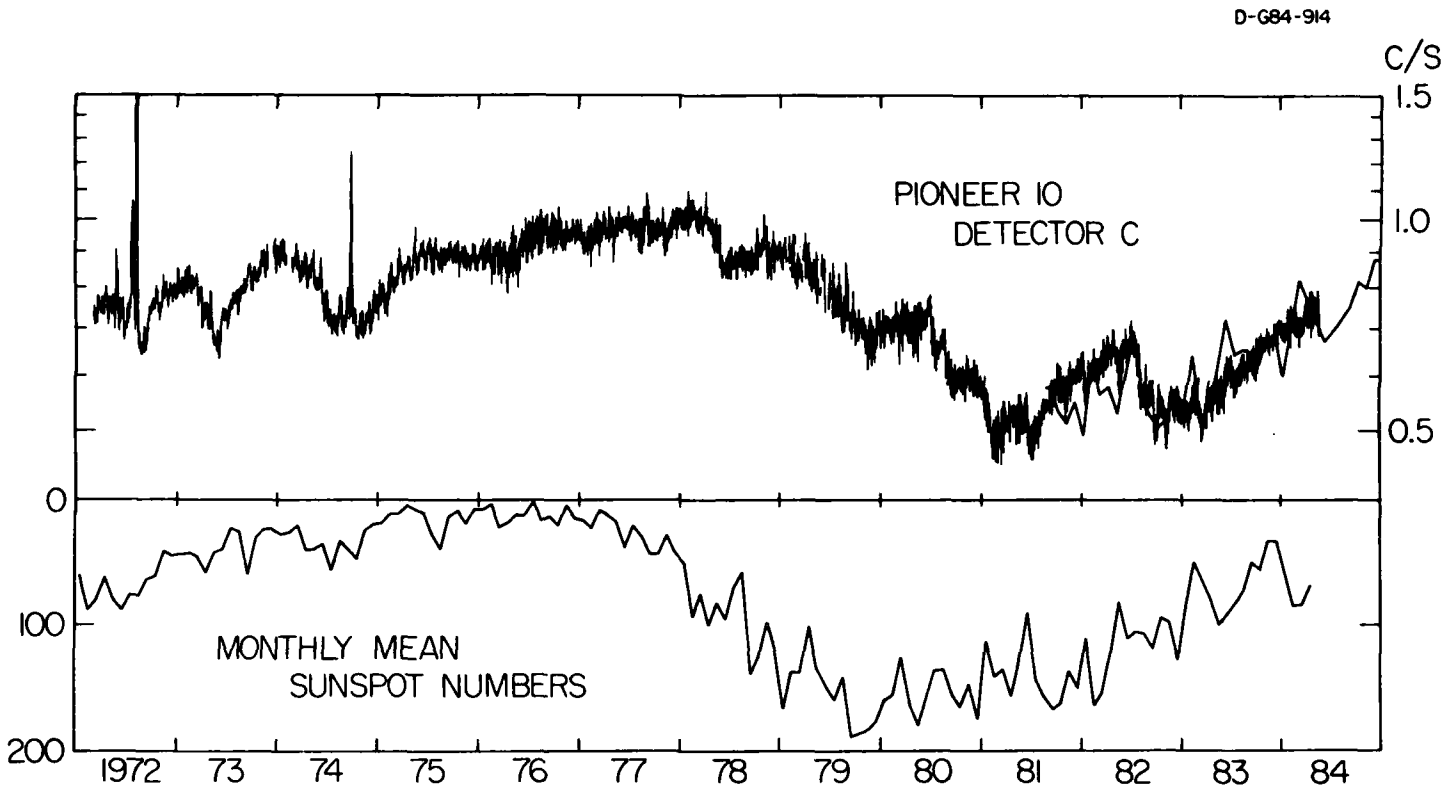
D-G84-914
C/S
1.5
1.0
0.5
PIONEER 10
DETECTOR C
0
100
200
MONTHLY MEAN
SUNSPOT NUMBERS
1972
73
74
75
76
77
78
79
80
81
82
83
84

Figure 6

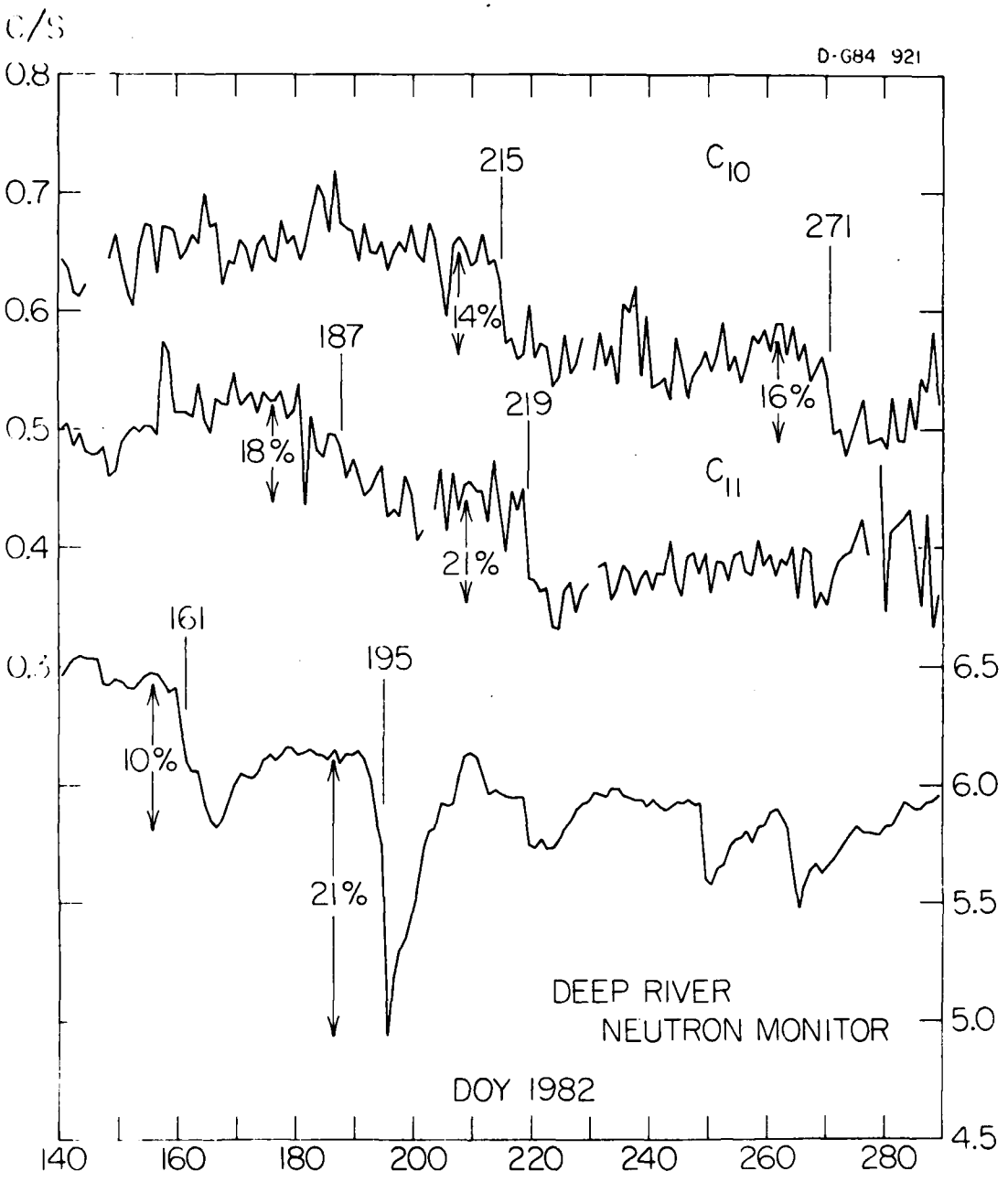
C/S
D-G84 921
0.8
0.7
0.6
0.5
0.4
0.3
215
C_{10}
271
14%
187
219
16%
18%
C_{11}
21%
161
195
10%
21%
6.5
6.0
5.5
5.0
4.5
DEEP RIVER
NEUTRON MONITOR
DOY 1982
140
160
180
200
220
240
260
280

Figure 7

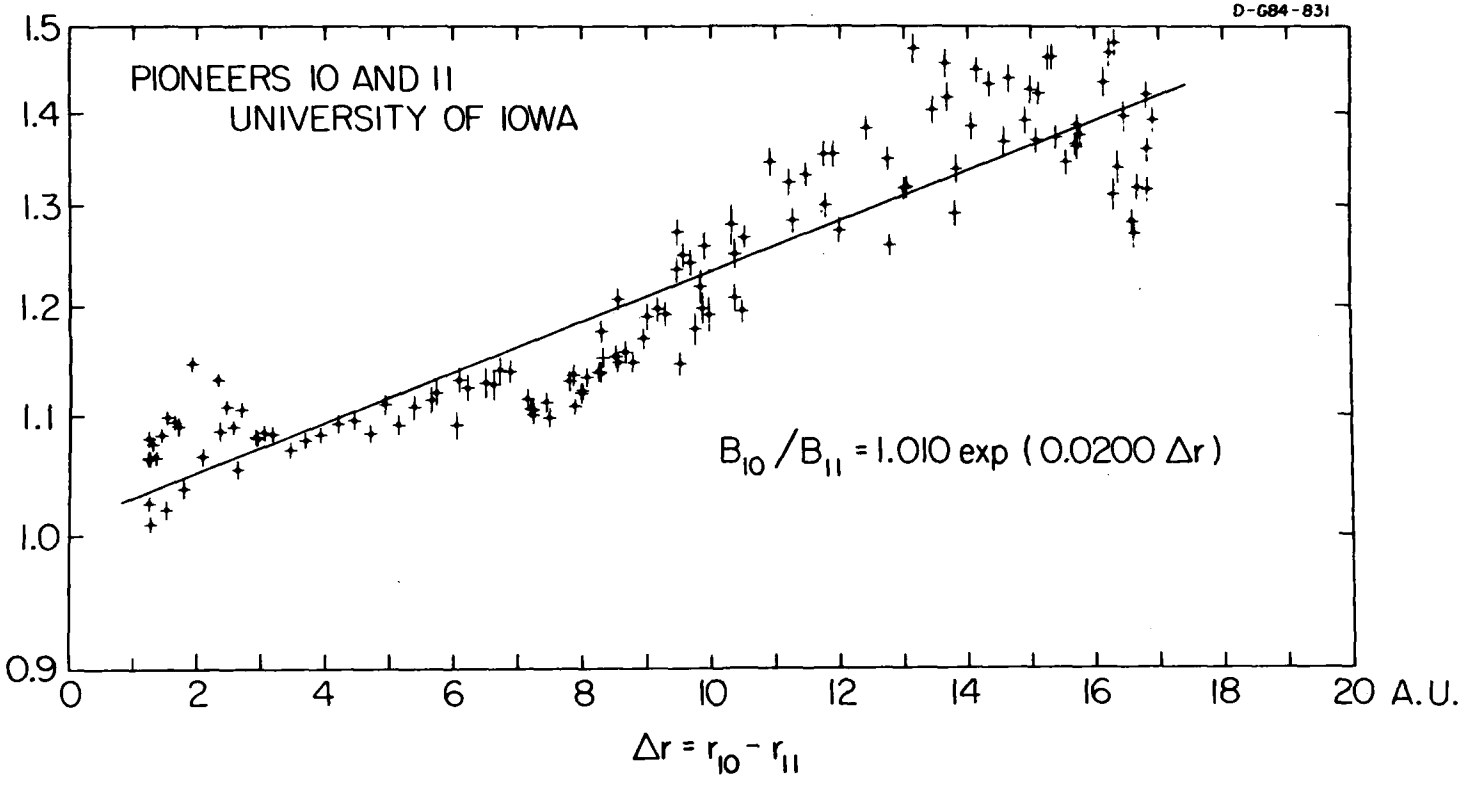
D-G84-831
PIONEERS 10 AND 11
UNIVERSITY OF IOWA
$B_{10}/B_{11} = 1.010 \exp(0.0200\,\Delta r)$
1.5
1.4
1.3
1.2
1.1
1.0
0.9
0
2
4
6
8
10
12
14
16
18
20 A.U.
$\Delta r = r_{10} - r_{11}$

Figure 8

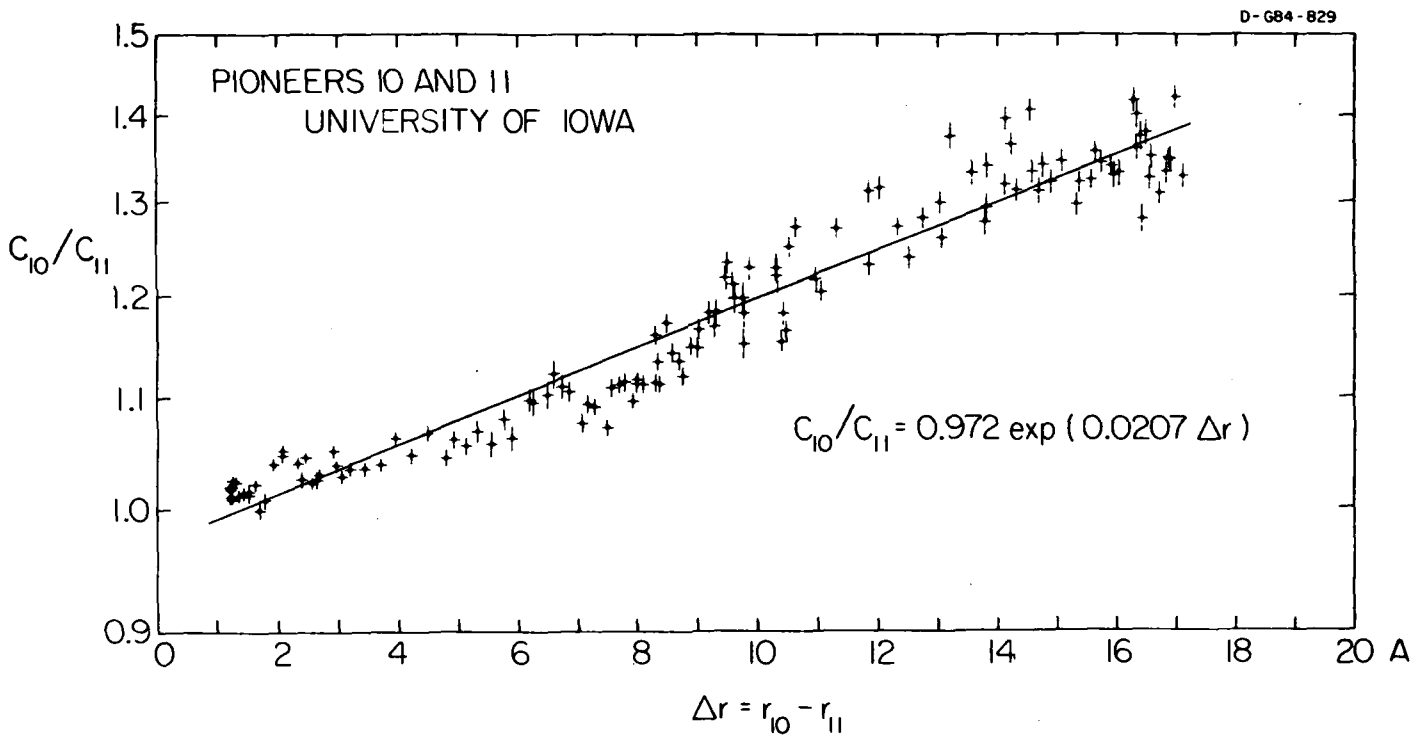
D-G84-829
PIONEERS 10 AND 11
UNIVERSITY OF IOWA
C_{10}/C_{11}
$C_{10}/C_{11} = 0.972 \exp(0.0207 \Delta r)$
$\Delta r = r_{10} - r_{11}$
1.5
1.4
1.3
1.2
1.1
1.0
0.9
0
2
4
6
8
10
12
14
16
18
20 A

Figure 9

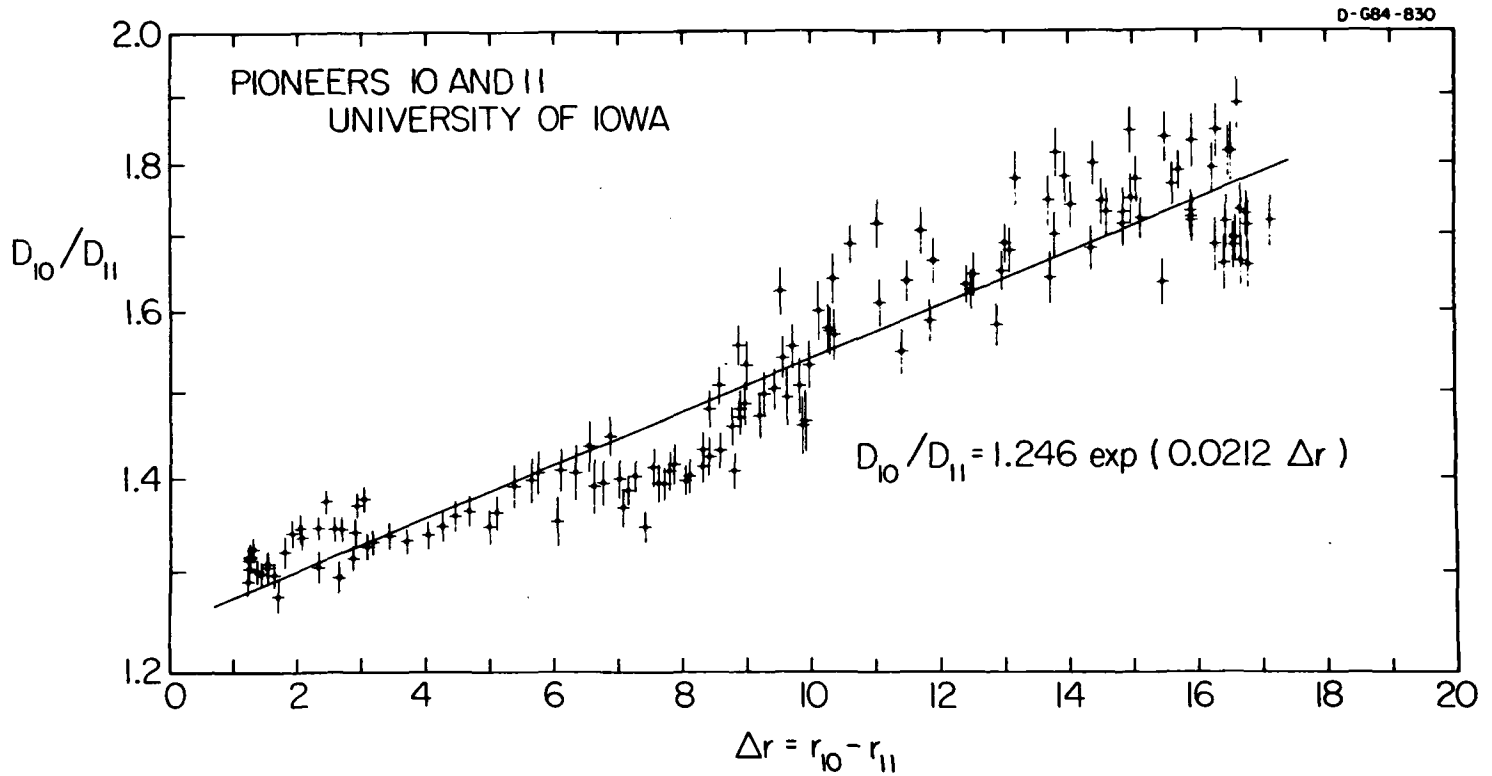
D-G84-830
PIONEERS 10 AND 11
UNIVERSITY OF IOWA
D_{10}/D_{11}
$D_{10}/D_{11} = 1.246 \exp(0.0212\ \Delta r)$
$\Delta r = r_{10} - r_{11}$
2.0
1.8
1.6
1.4
1.2
0
2
4
6
8
10
12
14
16
18
20

Figure 10

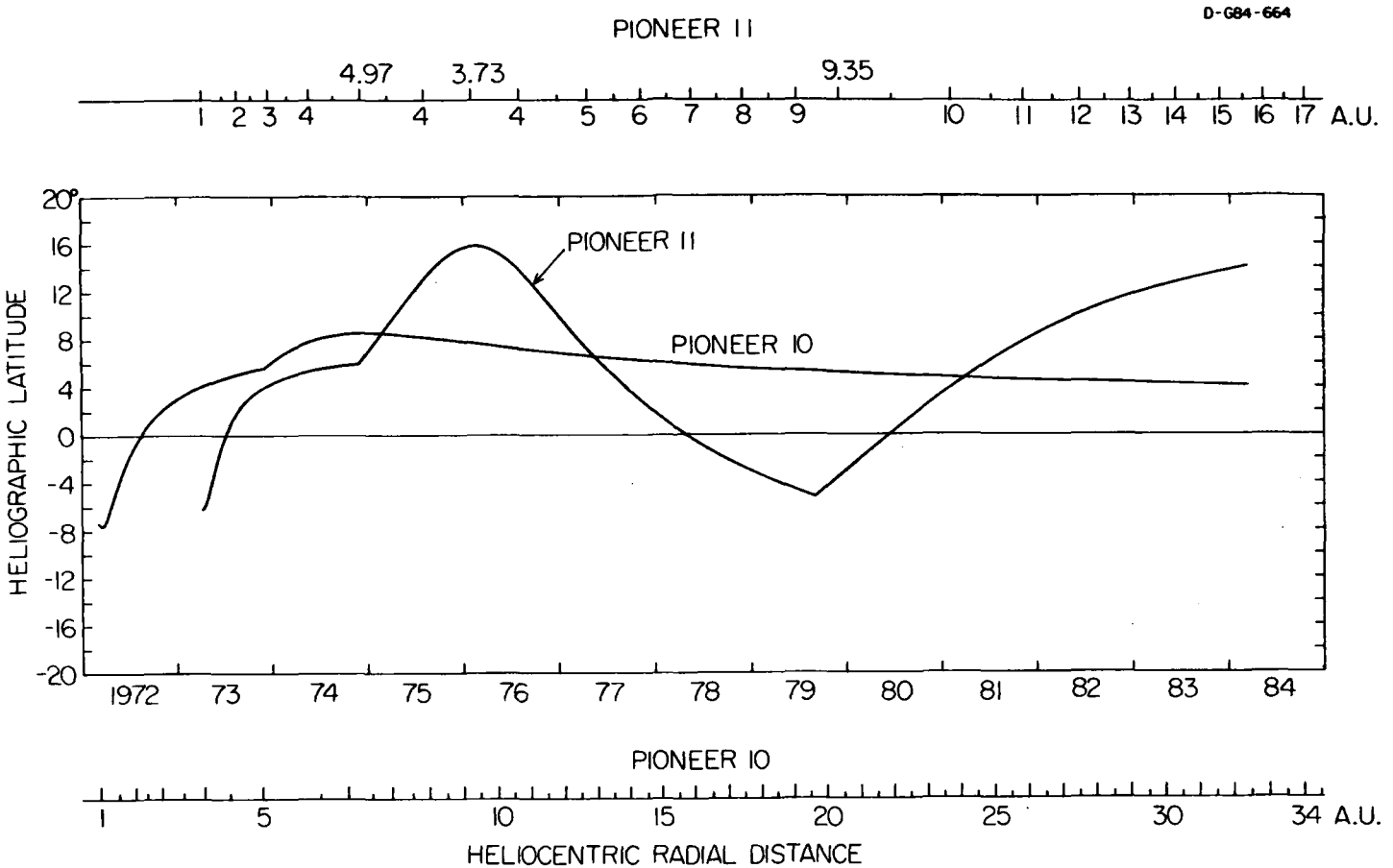
D-G84-664
PIONEER 11
4.97
3.73
9.35
1 2 3 4 4 4 5 6 7 8 9 10 11 12 13 14 15 16 17 A.U.
20°
16
12
8
4
0
-4
-8
-12
-16
-20
HELIOGRAPHIC LATITUDE
PIONEER 11
PIONEER 10
1972 73 74 75 76 77 78 79 80 81 82 83 84
PIONEER 10
1 5 10 15 20 25 30 34 A.U.
HELIOCENTRIC RADIAL DISTANCE

Figure 11

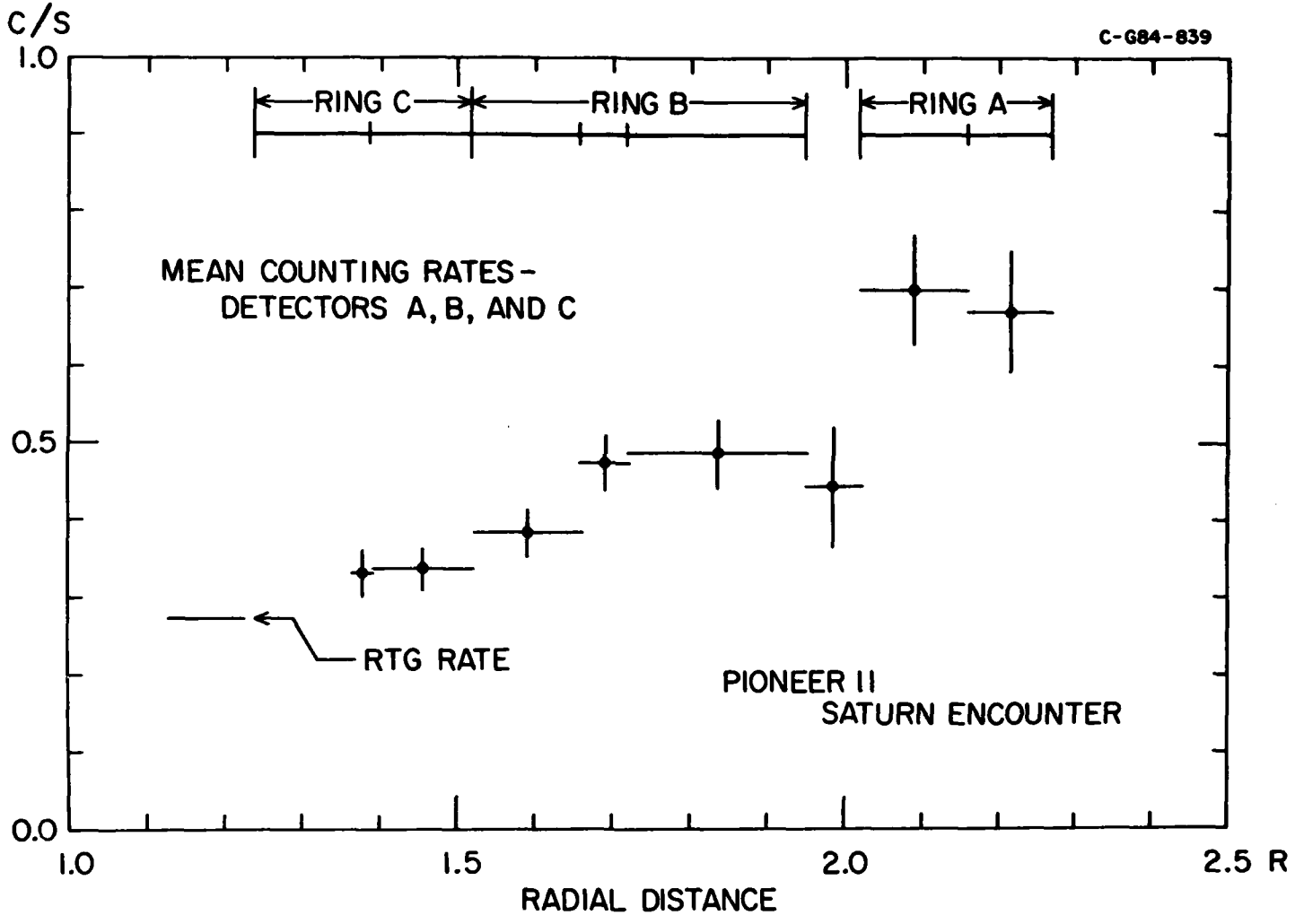
C/S
C-G84-839
1.0
0.5
0.0
RING C
RING B
RING A
MEAN COUNTING RATES -
DETECTORS A, B, AND C
RTG RATE
PIONEER 11
SATURN ENCOUNTER
1.0
1.5
2.0
2.5 R
RADIAL DISTANCE

Figure 12

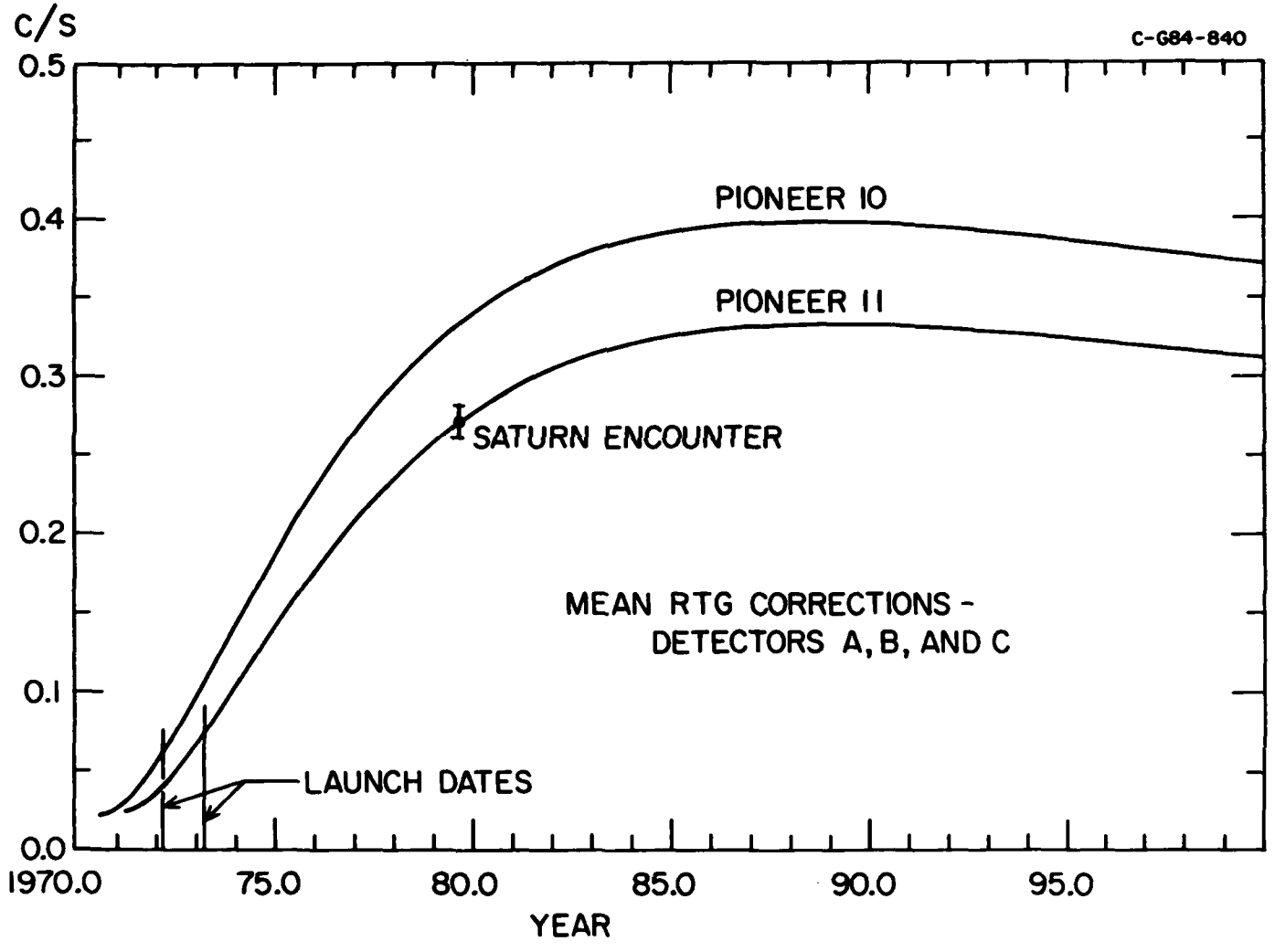
C/S
C-G84-840
0.5
0.4
0.3
0.2
0.1
0.0
PIONEER 10
PIONEER 11
SATURN ENCOUNTER
MEAN RTG CORRECTIONS -
DETECTORS A, B, AND C
LAUNCH DATES
1970.0
75.0
80.0
85.0
90.0
95.0
YEAR

Figure 13

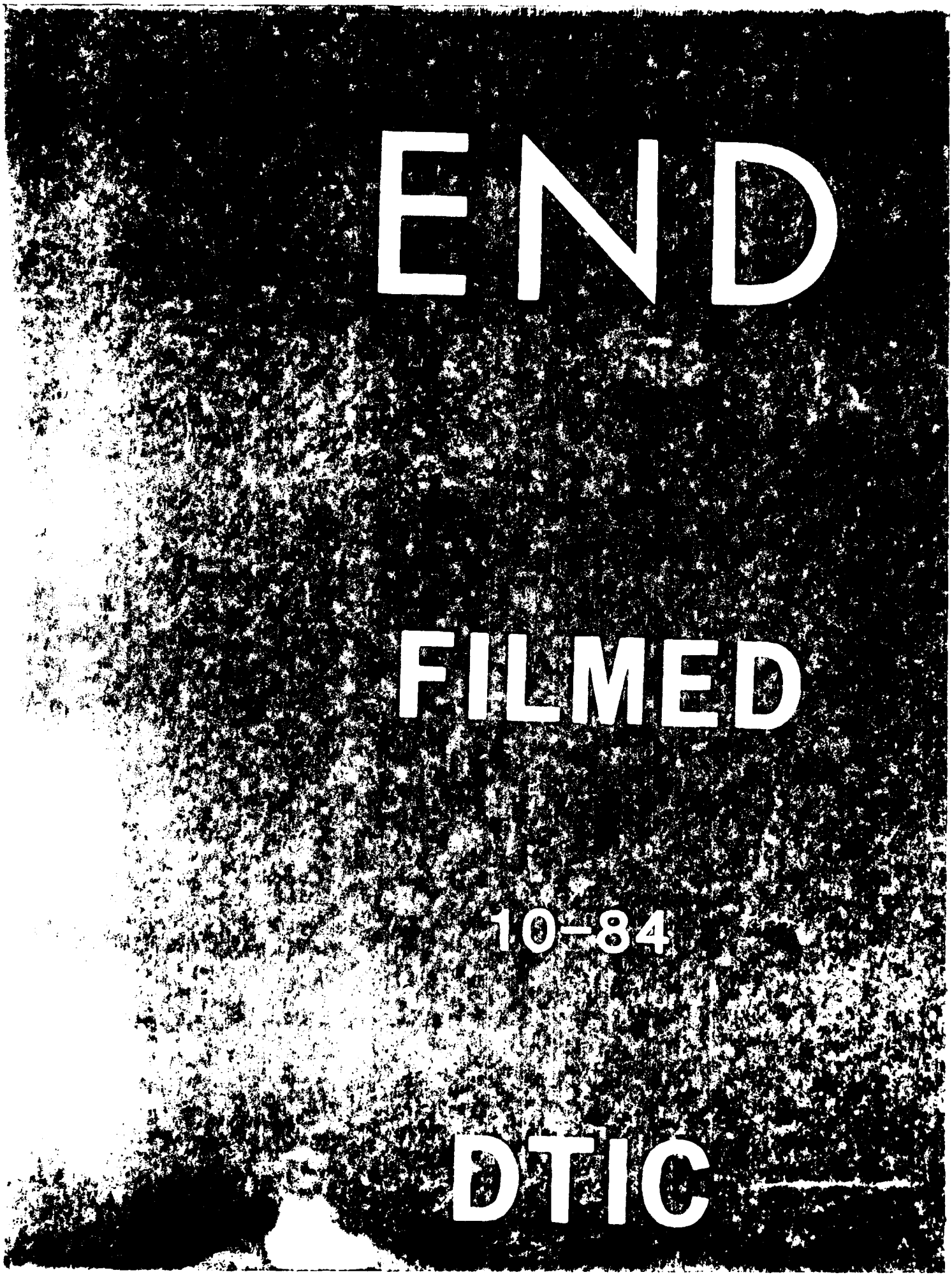
END
FILMED
10-84
DTIC